A POLY-N-ISOPROPYLACRYLAMIDE BASED HYDROGEL AS A NOVEL MATERIAL FOR VITREOUS REPLACEMENT

A POLY-N-ISOPROPYLACRYLAMIDE BASED HYDROGEL AS A NOVEL MATERIAL FOR VITREOUS REPLACEMENT

By

ROBYN PERRY, B. Sc.

A Thesis

Submitted to the School of Graduate Studies

In the Partial Fulfillment of the Requirements

For the Degree

Master of Applied Science

McMaster University

MASTER OF APPLIED SCIENCE (2013) Hamilton, Ontario

(Chemical Engineering) McMaster University

TITLE: A poly-N-isopropylacrylamide based hydrogel as a novel material for vitreous replacement

AUTHOR: Robyn Perry, B.Sc.

SUPERVISOR: Professor Heather Sheardown

NUMBER OF PAGES: ix, 87

Abstract

Although improvements in vitreous replacement technologies have lead to more desirable outcomes in patients with vision problems such as retinal detachment and vitreous hemorrhage, there remain a number of issues with current approaches. Many common therapies are limited to specific cases, or require extensive post-operative positioning, follow-up, and even secondary surgery for removal.

Thermally responsive materials composed of N-isopropylacrylamide, N-acryloxysuccinimide, and poly(ethylene glycol) were obtained through free-radical polymerization and were examined for the potential for use as artificial vitreous replacements. While in solution these materials were capable of transitioning from free-flowing liquids at room temperature to viscous solutions at physiological temperatures. Solutions of these materials were shown to have refractive indices similar to currently used vitreous replacements and gel-like mechanical properties at 37^{o}C. Optical transparency studies were performed and most samples displayed adequate transmittance values in the visible spectrum. Co-monomer content and molecular weight were found to have an effect on the temperature of the phase transition, as well as the transparency and cellular compatibility of the solutions at 37^{o}C.

While the materials studied require further optimization, these results suggest that poly(N-isopropylacrylamide) based polymers may have potential for use in vitreous replacement therapies.

Acknowledgements

I would like to express my gratitude to Heather Sheardown for giving me the opportunity to work in her lab and for all of her guidance and support throughout the past few years.

I'd also like to thank the members of the Sheardown lab for all of their help, whether they were simply giving suggestions or passing along their wealth of knowledge. This experience would not have been the same without their assistance. Thanks also to the Adronov, Stöver, and Hoare labs, as well as the Centre for Microbial Chemical Biology, for lending me their equipment and expertise.

And finally, to my family and friends, thank you for your constant encouragement and support.

TABLE OF CONTENTS

LIST OF FIGURES

LIST OF TABLES

1.0 Introduction

Advances in vitreous replacement technology have led to improvements in the prognosis of vision problems such as retinal detachment and vitreous hemorrhage. Although these problems are not commonplace, with retinal detachment affecting only 1 in 300 people in their lifetime (Turner 2010), left untreated, they can severely impact a patient's quality of life. As the incidence of these issues also tends to increase with age, the number of expected cases in the developed world is expected to as the age of the general population increases.

Though vitreous replacements have advanced considerably since their beginnings as air and basic physiological solutions, the most recent advancement in the field that went on to become a commonplace treatment was the introduction of silicone oil in the 1970's. Because vitrectomy and subsequent vitreous replacement is not as frequently performed as other ocular surgeries, there remain a number of unaddressed issues with current approaches. Most vitreous replacement therapies are unsuitable for all but a few very specific applications, and many require postoperative positioning, follow-up, or secondary surgery for removal.

The most promising materials for vitreous replacement at present appear to be hydrogels either directly injected or crosslinked once in place inside the eye. However, in-situ crosslinking may require the presence of a chemically active reagent that can cause damage to nearby tissues, and direct injection can result in fragmentation of the gel and a

subsequent loss of mechanical stability. Furthermore, removal would be difficult. Therefore, thermally activated gelation may be an attractive feature of novel vitreous replacement materials. Previous work has shown that PNIPAAm-based materials in solution are capable of transitioning from a liquid state to an optically transparent gel. These materials have also been shown to be highly biocompatible (Fitzpatrick 2012). The objective of the current work is to develop a novel polymer using PNIPAAm as a backbone to provide a long-term, non-toxic vitreous replacement material. Using a standard free-radical initiated polymerization, NIPAAm-containing polymers were prepared and relevant characteristics such as transparency, refractive index, viscosity, and interaction with retinal epithelial cells were studied to assess the potential of these materials for vitreous replacement applications.

2.0 Literature Review

2.1 Anatomy of the Eye

The eye serves to convert light from the surrounding environment into a nervous signal, which is interpreted by the brain. Light first passes through the cornea, the protective layer of cells that compose the anterior surface of the eye. It then travels through the aqueous humour, and the iris, which regulates the amount of light that reaches the deeper regions of the eye. Light then passes through the lens, and is focused on the posterior eye. This focusing action is controlled by the ciliary body, which sits behind the iris and is also responsible for the secretion of aqueous humour. The ciliary body is divided into the pars plana posteriorly and the pars picata anteriorly. Before light can reach the back of the eye it must pass through the vitreous humour, often referred to simply as the vitreous, a large transparent structure that maintains the shape of the eye. At the retina in the back of the eye, a thin layer of photosensitive cells converts light into a nervous signal. These cells exist in the highest concentration in an area called the macula, near the center of the retina. It is this area on which the lens focuses the light, and which is responsible for the central portion of vision. The nervous signal generated by these cells is transported to the brain via the optic nerve. The area where the optic nerve leaves the eye, often referred to as the optic disc, contains no light-sensitive cells. The location of these structures is laid out in the diagrams below.

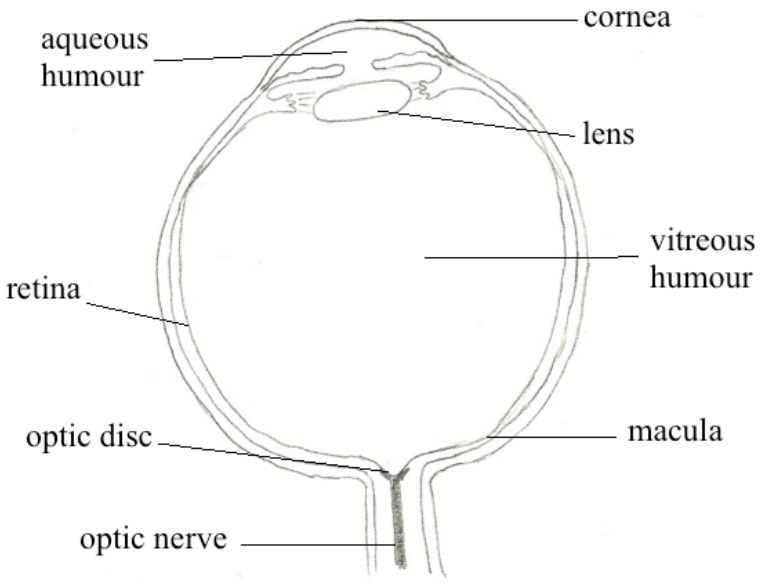

Figure 1. Diagram showing transverse cross-section of eye (Adapted from Worst and Los, 1995)

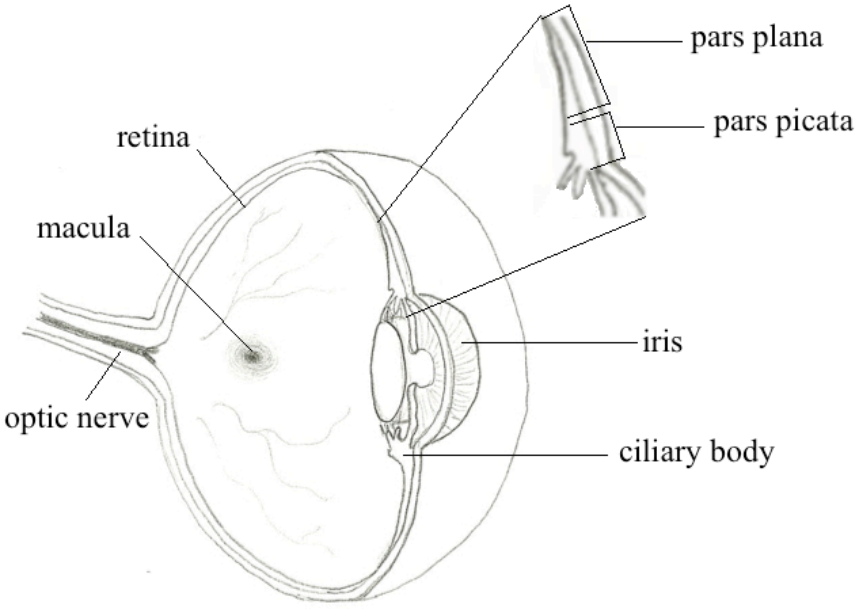

Figure 2. Diagram showing sagittal cross-section of eye (Adapted from Worst and Los, 1995)

2.1.1 Anatomy of the Vitreous

The vitreous humour is the largest structure in the eye by volume, occupying approximately 4.5 mL in the average adult human (Jongebloed, Humalda and Worst 1986) (Bishop 2000). While the nature of the vitreous has been difficult to study due to the challenge of in vivo assessment and the tendency of the structure to liquefy post-mortem (Nickerson, et al. 2008), the chemical morphology has been relatively well determined. By weight, the vitreous is composed of approximately 99% water and 0.9% salts (Bishop 2000). The remaining 0.1% by weight consists of structural proteins and polysaccharides, including collagen and hyaluronic acid (Bishop 2000). It has been shown that the collagen fibrils present in the vitreous provide a stabilizing scaffold (Bos, et al. 2001), but the purpose of the other large molecules is less well understood. While it has been demonstrated that hyaluronic acid associates with the collagen fibres that make up the vitreous network (Nishikawa and Tamai 1995), the role that this association plays is still unclear. It has been hypothesized that these polysaccharides may impart shock-absorbing properties (Chirila, et al. 1998). Other theories suggest that aggregated hyaluronan and sulphated proteoglycans may attach to multiple collagen fibrils via protein cores, serving to hold the network together (Scott 1992).

Despite the challenges of examining the vitreous, a number of anatomical regions within the structure have been defined. These regions include the central vitreous, the basal vitreous, and the vitreous cortex (Bishop 2000). Each of these regions appears to contain a unique arrangement of collagen fibrils. The central vitreous comprises the bulk of the vitreous body. This region is characterized by sparse collagen fibrils that tend to run from

the vitreous cortex in the posterior of the region to the basal vitreous in the anterior of the region (Sebag 1987). The basal vitreous lies over the junction of the retina and the pars plana, and the collagen fibres in this region tend to be very densely packed and firmly adherent to both underlying structures (Bishop 2000). The vitreous cortex also has a much higher collagen concentration than the central vitreous; this region is a thin layer that surrounds the central vitreous and is often divided into anterior and posterior segments (Bishop 2000). The anterior segment comes forward from the pars plana to cover the posterior surface of the lens, and is in direct contact with the aqueous humour (Bishop 2000). The posterior segment of the vitreous cortex covers the inner surface of the retina, but is absent over the optic disc and the macula (Sebag and Balasz 1989). Fibres in these regions tend to run parallel to the surface, and in the case of the posterior cortex may be indirectly attached to the retina (Bishop 2000).

2.1.2 Role of the Vitreous

A number of physiological functions have been ascribed to the vitreous gel. Primary functions include its role as a conduit for the metabolic needs of the lens, providing support for the retina, and its maintenance of transparency by excluding larger cells and molecules from the vitreal cavity (Le Goff and Bishop 2008). It has also been suggested that the vitreous may play an important role in inhibiting angiogenesis to maintain clarity (Holekamp 2010) and protecting other structures in the eye during mechanical trauma (Bishop 2000). While these functions may not be exclusively attributed to the vitreous, vitreal dysfunctions such as opacification, liquefaction, or physical collapse have been connected to many disorders in the surrounding tissues (Baino 2011).

2.2 Disorders of the vitreous

2.2.1 Liquefaction and posterior vitreous detachment

As humans age, the vitreous adopts a more liquid structure (Sebag 1987). Evidence of liquid vitreous is present by 4 years of age, and by adulthood approximately 20% of the vitreous is liquid (Le Goff and Bishop 2008). While vitreous liquefaction has been well documented, the mechanisms underlying the progression are not clear. Liquefaction begins around the same time as the formation of macroscopic collagen fibers in the central vitreous, and it has been hypothesized that the two events may share a root cause (Bishop, Holmes, et al. 2004). This theory suggests that, during the aging process, the fibrils scattered throughout the vitreous begin to aggregate, resulting in a redistribution of collagen that ultimately leads to higher liquid content in specific areas of the vitreous (Akiba, Ueno and Chakrabarti 1994). It has been observed that the collagen fibrils of the vitreous tend to lose certain surface proteoglycans with age, which may predispose them to fusion when they come in contact with similarly exposed fibrils (Bishop, Holmes, et al. 2004). It has also been demonstrated that free radicals generated by light irradiation may crosslink vitreous collagen and degrade hyaluronic acid, which could also contribute to aggregation and insolubilization of collagen fibrils (Akiba, Ueno and Chakrabarti 1994). Other studies suggest that liquefaction may be unrelated to the precipitation of vitreous collagen, instead demonstrating that a breakdown of vitreous collagen occurs during the aging process (Los, et al. 2003). This breakdown could result in a destabilization of the vitreous matrix and ultimately lead to liquefaction.

While vitreous liquefaction may not change the optical properties of the eye, it can still negatively impact vision due to the tendency for the liquefied vitreous to detach from the retina (Sebag 1987). Posterior vitreous detachment occurs when the liquefied portion of the vitreous seeps out of one of the holes in the vitreous cortex, most often above the macula (Bishop 2000). This liquid interferes with the attachment of the cortex to the retina and can ultimately result in complete detachment (Bishop 2000). Posterior vitreous detachment leaves the retina unsupported, which often leads to retinal damage in the form of tears, and subsequent retinal detachment as fluid accumulates between the layers of retinal tissue (Chirila, et al. 1998). This type of retinal detachment is referred to as rhegmatogenous retinal detachment, though retinal detachment can also result from complications unrelated to vitreous liquefaction.

2.2.2 Vitreoretinopathy

One serious complication of retinal detachment is known as proliferative vitreoretinopathy. This condition is characterized by the migration of retinal cells that normally reside under the surface of the retina. These cells escape through retinal tears and begin to proliferate, both on the surface of the retina and on the anterior of the vitreous (Pastor 1998). The cells can form sheets which exert contractile forces on the retina, resulting in visual distortion and often enlarging or maintaining retinal tears which can lead to recurrent or progressive retinal detachment (Leaver 1995). Surgical treatment for milder forms of proliferative vitreoretinopathy is very similar to that for rhegmatogenous retinal detachment, but with additional steps to remove the newly-formed membranes. More severe forms of this disorder require more complex forms of

surgical intervention, sometimes including partial removal of the retina (Pastor 1998). In all cases, the rate of success for retinal reattachment after proliferative vitreoretinopathy is around 70%. Visual success is significantly lower, with less than 60% of patients regaining visual acuity of more than 5/200 (Pastor 1998). Although it has been proposed that the best prevention for proliferative vitreoretinopathy is the successful treatment of initial retinal detachment (Leaver 1995), effective treatment options must still be developed as this condition can also occur as a complication of ocular trauma (Cardillo, et al. 1997).

Although proliferative vitreoretinopathy is the most prevalent type of vitreoretinopathy, other kinds exist. Familial exudative vitreoretinopathy is a genetic disorder, which results in a condition with characteristics similar to those of proliferative vitreoretinopathy. Patients with this condition will develop thick, fibrovascular vitreous membranes that pull on the retina, leading to visual distortion, and in certain cases, to progressive retinal deterioration and retinal detachment (Benson 1995). Although the long-term value of treatments for this disease remain uncertain, it has been shown that surgical intervention including vitrectomy can successfully restore some of the vision loss associated with the condition (Benson 1995).

2.2.3 Vitreous hemorrhage

The vitreous can also be affected by trauma to, or disease in, the surrounding tissues. Because the vitreous is mostly free of cellular activity, it can take several weeks for foreign material to clear (Shaw Jr and Landers 3rd 1975). Vitreous hemorrhage occurs when one of the surrounding tissues releases blood into the vitreous. In young people, the

leading cause of vitreous hemorrhage is simple trauma (Lindgren, Sjödell and Lindblom 1995). In adults, vitreous hemorrhage is often related to diabetic retinopathy, where angiogenesis of weak blood vessels can result in the leakage of large amounts of blood into the vitreous cavity (Lindgren, Sjödell and Lindblom 1995). The leading cause of vitreous hemorrhage, however, appears to be vitreous detachment and subsequent retinal traction (Lindgren, Sjödell and Lindblom 1995). Hemorrhage can also occur as a result of retinal tearing, macular degeneration, or certain retinopathies (Lindgren, Sjödell and Lindblom 1995).

In mild cases, vitreous hemorrhage may be treated with rest to allow the blood to settle until it can be cleared by natural processes. In more severe cases, however, vitrectomy may be necessary to remove the blood after the underlying condition has been treated (Shaw Jr and Landers 3rd 1975).

2.3 Vitreous Replacement

In order to maintain hydraulic pressure in the vitreous cavity after removal of the vitreous or during certain surgical procedures, some material must be used as a vitreous replacement. The requirements of these materials may vary depending on usage; something intended for use as a short-term tamponade during a surgical procedure may have less stringent requirements than those intended as longer-term vitreous replacements (Baino 2011). Materials used in, or being evaluated for use in, these capacities include gases, liquids, natural and synthetic polymers, and various hydrogel systems.

2.3.1 Gases

Gases are frequently used as short-term vitreal tamponades, such as during surgery for certain types of retinal detachment (Han, et al. 1998). These materials are easily injectable and undergo good expansion in the eye, effectively maintaining intraocular pressures with very little injectable material (Soman and Banerjee 2003). However, they may contribute to such pathologies as lens opacification and result in histopathological changes to the ocular tissues (Soman and Banerjee 2003), as well as increased intraocular pressure that can lead to damage of the optic nerve (Baino 2011). These materials also require postoperative positioning and the avoidance of significant changes in pressure, such as those experienced during air travel (Chang, et al. 2003). It has also been demonstrated that they are ineffective for certain applications, such as the closure of inferior retinal holes (Chang, et al. 2003).

2.3.1.1 Air

One of the first materials investigated as a vitreous substitute was air. This was first used in 1911 to treat a case of rhegmatogenous retinal detachment (Baino 2011). However, air has a residence time in the globe of only a few days (Soman and Banerjee 2003), and is therefore unsuitable as a long-term vitreous replacement.

2.3.1.2 Sulfur hexafluoride

Sulfur hexafluoride has been in use as an ocular tamponade since the 1970s (Hakin, Lavin and Leaver 1993). As an alternative to air, sulfur hexafluoride has a number of advantages, including the ability to expand up to twice its volume to exert a better tamponade effect (Soman and Banerjee 2003). The residence time of this gas is also

longer than that of air, although at only 2 weeks, it is also unsuitable as a longer-term replacement (Soman and Banerjee 2003).

2.3.1.3 Perfluorocarbons

Introduced in the 1980s as a replacement to sulfur hexafluoride, perfluorocarbons are a class of compounds that contain only carbon and fluorine (Soman and Banerjee 2003). Perfluorocarbons currently in use include perfluoropropane and perfluoroethane, although perfluoropropane is more widely used (Baino 2011). These compounds can expand to up to four times their volume and are reabsorbed more slowly than sulfur hexafluoride; they are able to maintain a tamponade effect for up to 1 week (Soman and Banerjee 2003). The residence time of these materials can be up to two months depending on the specific perfluorocarbon used (Baino 2011). However, some evidence has shown that these materials may cause damage to the ciliary body and other tissues (Sparrow, et al. 1990).

2.3.2 Liquids

2.3.2.1 Physiological solutions

Among the first liquids to be injected into the vitreous cavity were water and balanced salt solutions. (Baino 2011). Because of their low viscosity and short intravitreal residence time, use of these liquids results in an inadequate tamponade effect (Baino 2011). However, these liquids are still used in ocular surgery for the removal of other tamponade agents, such as silicone oil and perfluorocarbon liquids (Baino 2011).

2.3.2.2 Silicone oils

Silicone oils were first investigated for the treatment of retinal detachment in the early 1960s and gained widespread acceptance in the 1970's (Baino 2011); in spite of this, silicone oils only gained FDA approval in 1994 (Soman and Banerjee 2003). Most silicone oils used in ocular surgery are simple polydimethylsiloxane (PDMS) with molecular weights ranging from 40 to 70 kDa (Soman and Banerjee 2003). In practice, silicone oils are differentiated by viscosity, with higher molecular weight values correlating to higher viscosity materials. The most widely used silicone oil for vitreal replacement is 5000 cSt PDMS (Baino 2011) as this is the highest viscosity material that can be effectively injected into the back of the eye through a reasonably sized needle. These materials are useful for patients who cannot be positioned after the injection of gases, those who must travel by air, and those with monocular vision (Goldbaum, et al. 1998). They are the preferred choice of treatment for long-standing rhegmatogenous retinal detachment, retinal detachment caused by proliferative diabetic retinopathy, and giant retinal tears (Baino 2011). However, they are not useful for the treatment of inferior retinal breaks because of their tendency to float on the residual vitreal fluid (Baino 2011), and their hydrophobic nature means that they cannot fully fill the vitreal chamber, resulting in a less effective tamponade (Soman and Banerjee 2003). Additionally, there may be toxic effects related to oil impurities and lower molecular weight components, as well as those related to emulsification and dispersion of the oil (Baino 2011). Using higher viscosity oils may ameliorate these effects (Heidenkummer, Kampik and Thierfelder 1991), although hydrophobic properties may increase and injection becomes

more difficult with increasing viscosity. It has been shown that the use of silicone oils as a longer-term vitreous replacement can also lead to cataract, glaucoma, and corneal damage (Baino 2011). For this reason, surgical removal of the material is necessary. Additional risks are present with surgical removal; for example, the risk of retinal detachment following removal of silicone oil is greatly increased (Baino 2011).

2.3.2.3 Fluorosilicone oils

Second-generation silicone oils with fluorinated siloxane groups have been investigated to overcome the shortcomings of conventional silicone oils in treating conditions such as inferior retinal breaks. These materials may consist either of a repeating fluorosilicone group or be copolymerized with dimethylsiloxane (Sparrow, et al. 1990). Due to their higher density, these oils can be successfully used in the treatment of inferiorly or posteriorly located retinal tearing (Baino 2011). However, these materials are less well-tolerated than regular silicone oil; it has been observed that complications associated with regular silicone oil occur within a shorter time period with the use of fluorosilicone oils, possibly due to the higher emulsification rates of these newer materials (Baino 2011).

2.3.2.4 Magnetic silicone oils

Even newer materials being investigated include magnetic silicone oils: silicone-based oils containing magnetic compounds. These materials are capable of overcoming the hydrophobic nature of silicone oils to fully fill the vitreous by the use of a magnetic band around the eye (Dailey, et al. 1999). However, studies of such materials have revealed difficulties associated with heavy metal toxicity and removal of the magnetic band (Dailey, et al. 1999).

2.3.2.5 Semifluorinated alkanes and heavy oils

Other oils investigated as vitreal replacements include semifluorinated alkanes and heavy oils. Semifluorinated alkanes consist of short alkyl chains joined either at one or both ends to perfluorocarbon chains, while heavy oils consist of a mixture of semifluorinated alkanes and silicone oil (Baino 2011). These materials typically have lower viscosities, around 2.5 cSt, and have been used successfully in the treatment of retinal detachment, primary inferior rhegmatogenous retinal detachment, and persisting macular holes (Baino 2011). They exhibit reduced emulsification compared to silicone oils, but still present a risk of adverse events, such as cataract or glaucoma, with long term use (Baino 2011).

2.3.3 Polymers and hydrogels

More recently, a number of vitreous replacements based on long-chain polymers and hydrogel systems have been studied. These materials may take one of two approaches; they will either attempt to mimic the composition and structure of the native vitreous, or disregard the native structure and attempt to mimic the features of the vitreous (Baino 2011).

Materials that attempt to mimic the composition generally consist of a mixture of collagen and hyaluronic acid, as these are the two components most prevalent in the native vitreous, and are involved in the most important structural interactions (Bishop 2000). However, attempts to reproduce the natural interactions between these molecules have not been successful. Simple mixtures of the two molecules exhibit low intravitreal residence time, while attempts to chemically crosslink the agents result in aggregation (Soman and Banerjee 2003). Both collagen and hyaluronic acid have been investigated

individually for their suitability as vitreous substitutes, but present similar barriers to efficacy (Stenzer, et al. 1969) (Schramm, et al. 2012). Hyaluronic acid in its natural form is quickly degraded in the eye, while cross-linked gels can remain for up to 6 weeks but may cause toxic effects in the retinal tissues (Schramm, et al. 2012).

Far more common have been efforts to reproduce the features of the native vitreous, either by using a simple polymer solution or by the use of injectable or in-situ crosslinked hydrogels. Simple polymer solutions include common hydrophilic polymers such as PEG, hydroxypropylmethylcellulose (HPMC) and polyvinyl pyrrolidone (PVP), while numerous hydrogel systems have been studied, including crosslinked networks of both PVP and polyvinyl alcohol (PVA) (Chirila, et al. 1998) (Maruoka, et al. 2006). High molecular weight PEG solutions have been evaluated as experimental vitreous replacements, but have been deemed unsuitable due to low retention times as well as the tendency for precipitates to form in vivo, despite good cellular compatibility and mechanical properties (Pritchard, et al. 2011). Solutions of both HPMC and PVP demonstrate short intravitreal residence times and rapid intraocular decreases in viscosity that render them incapable of providing an adequate tamponade (Soman and Banerjee 2003) (Baino 2011). Crosslinked PVP, however, has been shown to reside in the vitreous cavity for longer periods of time, although it may begin to biodegrade after extended periods (Soman and Banerjee 2003). Studies of crosslinked PVP as a vitreous substitute also demonstrate issues with both vitreous and corneal opacification, as well as an influx of inflammatory cells that contain granular material, presumably indicating phagocytosis of the gel (Chirila, et al. 1998). Crosslinked PVA also demonstrates potential as a vitreous

substitute, although some toxicity issues have been observed, possibly due to methods used in the manufacture of PVA (Maruoka, et al. 2006). Some opacification of the vitreous may also occur after implantation, especially if gels of higher viscosity are used (Maruoka, et al. 2006). This is likely due to fragmentation of the gels during the injection process. Such an outcome is unfortunate as those gels with higher viscosity provide a better tamponade effect. Polyacrylamide has also been studied as a vitreous replacement; despite the toxicity of acrylamide, its polymer form exhibits good compatibility with ocular tissues (Baino 2011). More recently, acrylamide has been crosslinked with thiol-containing compounds to allow the formation of disulfide crosslinks (Aliyar, et al. 2004). This procedure allows for more thorough removal of residual monomer, as well as allowing for the formation of a crosslinked gel. (Baino 2011).

Because of the tendency of pre-formed hydrogels to fragment under the shear stresses involved with injection, and the tendency of fragments to exacerbate toxicity issues, much research is currently involved with the concept of in-situ gellable materials. However, as cross-linking processes often involve reactive compounds or radical initiation, such materials may pose their own set of risks to the ocular tissues. Recently, thermally responsive polymer systems have been studied as an alternative to conventionally cross-linked gels.

2.4 Thermally responsive polymer systems

Many thermally responsive systems involve polymers that undergo changes in solubility as a response to increases in temperature. This response manifests at the so-called lower

critical solution temperature (LCST) and the effect is thought to result from a balance of hydrophobic and hydrophilic groups in the polymer chain (Hanyková, Labuta and Spěváček 2006). An increase in temperature can make interactions between water molecules and the polymer unfavorable, resulting in a conformational change as the polymer takes on a more hydrophobic structure (Hanyková, Labuta and Spěváček 2006). This conformational change is depicted below in Figure 3.

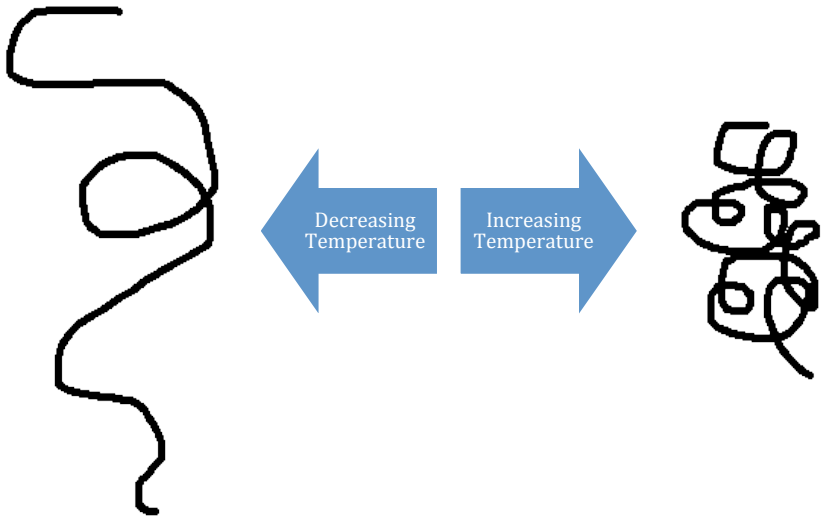

Figure 3. Temperature-dependent phase transition of thermosensitive polymer chains

Other thermally responsive systems can involve amphiphilic polymers that self-assemble into micelles in solution (Ruel-Gariépy and Leroux 2004). Some of these polymer micelles will pack together and form gels as temperature increases, due to the increasing favorability of polymer-polymer interactions over polymer-water interactions (Ruel-Gariépy and Leroux 2004).

2.4.1 Polysaccharides

Certain cellulose derivatives exhibit gel behavior upon heating. These compounds include HPMC, methylcellulose, and, with the addition of a surfactant, ethyl(hydroxyethyl)cellulose (EHEC). Aqueous solutions of both methylcellulose and HPMC gel upon heating, with methylcellulose forming an opaque gel between 40 and 50^{o}C, and HPMC transitioning between 75 and 90^{o}C (Ruel-Gariépy and Leroux 2004). The temperatures at which these phase transitions occur have also been successfully lowered through the addition of ionic salts to solution and through chemical modification of the hydroxypropyl groups of HPMC (Sarkar 2003). Methylcellulose-based gels have been investigated as tissue engineering scaffolds in certain applications. A 2001 study on the potential of such scaffolds for repair of traumatic brain injury showed good biocompatibility with both cultured cells and injured rat brains (Tate, et al. 2001). The main drawback for such gels in ocular applications is their poor transparency. EHEC in aqueous solutions can also exhibit temperature sensitive behaviour. Although it typically displays a decrease in viscosity as temperature increases (Carlsson, Karlström and Lindman 1990), the addition of an ionic surfactant to these solutions can reverse this behavior, resulting in gelation upon heating from room temperature to between 30 and 40^{o}C. (Carlsson, Karlström and Lindman 1990) Unfortunately, biocompatibility of such gels may be negatively affected by the inclusion of the ionic surfactant.

Xyloglucan is a naturally occurring polysaccharide found in the cell wall of plants and commercially isolated from tamarind kernels. Although native xyloglucan does not exhibit any gelation properties, partial degradation with beta-galactosidase results in a

polymer that undergoes a reversible phase transition upon heating (Shirikawa, Yamatoya and Nishinari 1998). The exact temperature of this transition will vary depending on the amount of galactose removal, and has been shown to occur at anywhere from 5 to 50^{o}C (Nisbet, et al. 2006), although most formulations studied in depth have shown transition temperatures between 22 and 27^{o}C (Nisbet, et al. 2006). Xyloglucan gels have been studied as delivery vehicles for several drugs and have shown both good tolerance in the tissues of interest, including ocular tissues (Miyazaki, et al. 2001), as well as increased bioavailability of the target drugs (Miyazaki, et al. 1998). Despite their many advantages, the relatively low transition temperature of most xyloglucan gels can pose challenges when handling at room temperature, and their optical properties have not been well characterized.

Chitosan is another polysaccharide that can form a thermally responsive gel in solution. A derivative of chitin, chitosan forms a gel in solution above pH 6.2 (Ruel-Gariépy, et al. 2000). The addition of polyol salts such as glycerophosphate has been shown to change this pH-based gelation to a temperature-sensitive one (Ruel-Gariépy, et al. 2000). Although studies of such gels have shown good cellular compatibility in vitro and in vivo with anterior segments of the eye (Chen, et al. 2011), there is still some loss of cell viability with retinal cells in vitro, and in vivo studies indicate high clearance levels which might render these materials unsuitable for vitreal replacement (Hsiao, et al. 2012).

2.4.2 Poloxamer systems

Thermosensitive poloxamer systems consist of non-ionic block copolymers composed of poly(ethylene oxide) (PEO) and poly(propylene oxide) (PPO) units in aqueous solutions.

The method of gelation for these systems is not well known, although the currently accepted hypothesis suggests that it occurs due to micellar formation as a result of PPO block dehydration above the critical micellization temperature (Ruel-Gariépy and Leroux 2004).

Poloxamers are used in a variety of industrial applications that take advantage of their surfactant-like qualities (Cabana, Aït-Kadi and Juhász 1992). They have also been widely investigated for various drug delivery applications. The most widely studied poloxamer system for biological applications is Poloxamer 407, which consists of a PPO block of molecular weight 4,000 $g \cdot mol^{-1}$ and has a PEO content of 70 weight percent (Cabana, Aït-Kadi and Juhász 1992). In solutions of 20%, this compound is a viscous liquid below 25°C but becomes a transparent gel upon heating to 37°C (Cabana, Aït-Kadi and Juhász 1992). In various studies Poloxamer 407 has been shown to increase the residence time of drugs administered parenterally, transdermally, rectally, vaginally and via ophthalmic pathways (Ruel-Gariépy and Leroux 2004). Although it is usually regarded as non-toxic, Poloxamer 407 may have systemic side effects. Studies have found that injections of Poloxamer 407 in rats and mice resulted in hypercholesterolemia and hypertriglyceridemia (Palmer, Emeson and Johnston 1998) (Wout, et al. 1992). Another potential drawback of Poloxamer gels is their rapid dissolution (Dumortier, et al. 2006).

Poloxamer has also been grafted with high molecular weight poly(acrylic acid) (PAA) in an effort to impart mucoadhesive properties to the polymer and further prolong residence time for drug delivery applications. Both Poloxamer grafted to PAA and PAA grafted to Poloxamer have been shown to form transparent gels at body temperature, at lower

concentrations than those required for the original Poloxamer system (Bromberg 1998). Such an effect may be advantageous as systemic effects are likely to be less severe with a lower administered dose. However, lower concentrations of Poloxamer in the gel may facilitate more rapid dissolution.

2.4.3 Thermosensitive liposomes

It is also possible to take advantage of thermally responsive micellar systems to deliver target molecules at certain temperatures. While such systems have largely been investigated in drug delivery and related applications, it has also been possible to use such systems to thermally trigger mineralization and gelation (Pederson, Ruberti and Messersmith 2003) (Westhaus and Messersmith 2001). In these systems, liposomes sequester reactive species until reaching a certain temperature, at which point the reactive species are released and the target reaction can take place. The reactive species used in thermosensitive liposome systems is frequently a bioactive ion such as calcium. These systems have successfully demonstrated the ability to rapidly form calcium crosslinked alginate gels as well as calcium-activated enzyme-catalyzed fibrinogen gels upon heating from room temperature (Pederson, Ruberti and Messersmith 2003). The major issue with such gels is of course their ionic content. In the case of alginate gels, multivalent calcium ions may be replaced with monovalent ions such as sodium in physiological conditions, effectively de-crosslinking the gel (Kikuchi, et al. 1997). The release of calcium may also have negative effects on nearby tissues (Orrenius, et al. 1992).

2.4.4 PNIPAAm

Poly(N-isopropylacrylamide) (PNIPAAm) is another polymer that undergoes a reversible phase transition at its LCST. What makes PNIPAAm an attractive polymer for biological applications is the fact that this phase transition occurs near physiological temperatures, as PNIPAAm's LCST is around 32^{o}C (Li, et al. 2005). Although toxicity issues are present with the monomeric form of this material, PNIPAAm is considered relatively biocompatible. A number of studies have been conducted on PNIPAAm's potential as a biomaterial, whether for cellular scaffolds or as a drug delivery agent. PNIPAAm and PNIPAAm-based polymers have been shown to support the growth of bovine articular chondrocytes, murine cardiosphere-derived cells, human bone marrow stromal cells, and leporine chondrocytes and meniscus cells for culture periods ranging from 1 week to 31 days (Stile, Burghardt and Healy 1999) (Li, et al. 2011) (Comolli, et al. 2009) (Chen and Cheng 2008). While these results are encouraging from a toxicity standpoint, the use of such materials as long-term vitreous replacements could pose problems if they allow for the proliferation of cells into the vitreous cavity, as this could lead to compromised vitreous clarity or even proliferative vitreoretinopathy. Recent work has also examined PNIPAAm-based materials for a number of ocular applications, including drug and cell delivery to the posterior segments of the eye (Fitzpatrick 2012). These materials have exhibited excellent tolerance with retinal cells in vitro and good tolerance when injected subcutaneously. Similar materials have also displayed excellent transparency characteristics, though these materials are degradable and are so unsuitable as longer-term vitreous replacements.

In the current work, we have attempted to take advantage of these characteristics in the design of a novel material for vitreous replacement. A PNIPAAm-based copolymer was designed using substituent groups selected for specific characteristics. While the majority of the polymer was composed of NIPAAm groups, PEG and N-acryloxysuccinimide (NAS) groups were also present. These co-monomers were selected for their demonstrated cellular compatibility in similar polymers (Fitzpatrick 2012), as well as for the chemical and structural characteristics they could impart. PEG was used in an attempt to increase the transparency of the material, as the longer, more hydrophilic side chains were expected to remain amorphous during the phase transition. The inclusion of NAS groups was intended to facilitate further work involving subsequent conjugation of these polymers to various molecules of interest. It was hypothesized that a thermally responsive system would ameliorate toxicity and opacification effects seen with fragmentation of injectable cross-linked gels while providing adequate physical support in the vitreous.

3.0 Materials and Methods

3.1 Polymerization

Unless otherwise stated, reagents were obtained from Sigma-Aldrich (Oakville ON). Materials were synthesized by free-radical polymerization at 70^{o}C in 1,4-dioxane. NIPAAm was purified by dissolution in toluene and recrystallization in n-hexane. PEG-methyl ether methacrylate with number-average molecular weights of 475, 950, and 1100 g/mol and acrylic acid n-hydroxysuccinimide ester were used without further purification. Dioxane was added to the dry reagents and the mixture allowed to dissolve at room temperature. Once the reagents were fully dissolved, benzoyl peroxide was added at 1 mole percent as a radical initiator. The solution was then purged with nitrogen gas for 15 minutes before being submerged in a 70^{o}C oil bath and allowed to react for 24 hours. The resulting polymers were precipitated in ethyl ether at room temperature and isolated by vacuum filtration. They were then re-dissolved in a small amount of tetrahydrofuran (THF) and precipitated again in ether. After filtration, the polymers were dried in a vacuum oven at 35^{o}C before undergoing testing for several key physical and chemical characteristics. For the sake of brevity, the name poly(NIPAAm-co-NAS-co-PEG) was abbreviated to PNNP$_{n}$, where n indicates the molecular weight of the PEG chain. A diagram of the chemical structures of the reactants and the resulting polymers is shown below.

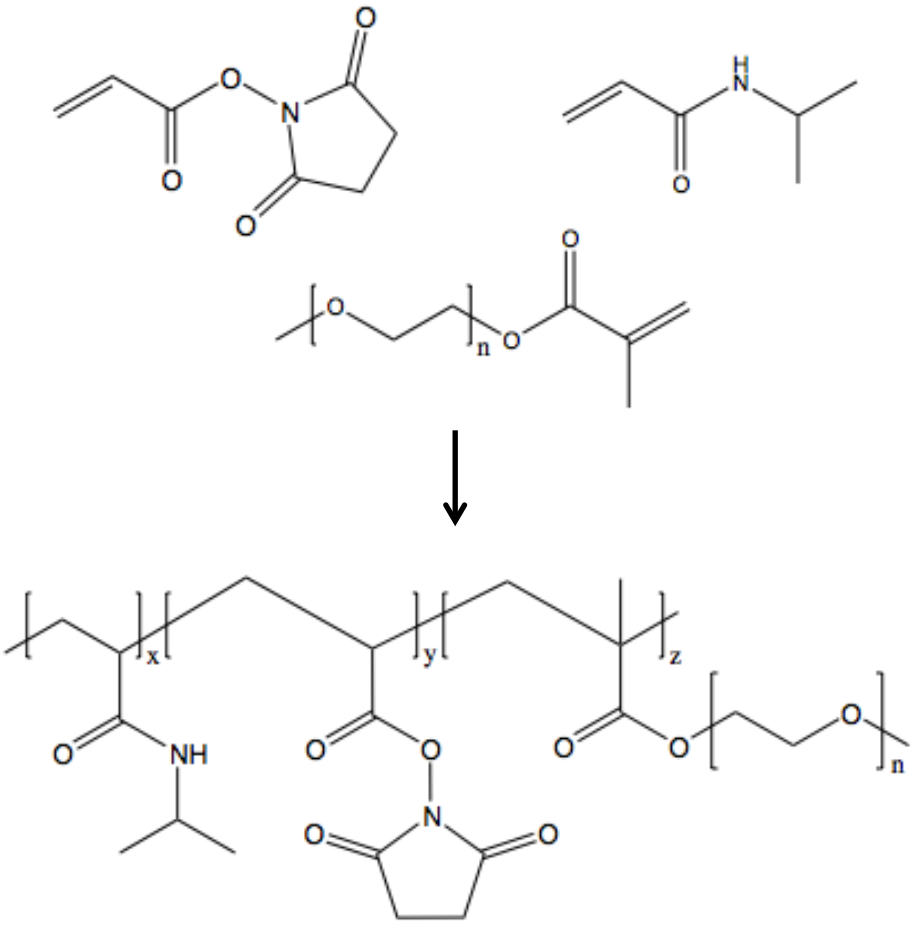

Figure 4. Chemical structure of $PNNP_n$

3.2 Polymer Characterization

3.2.1 Polymer composition

Verification of monomer ratios in the final polymer was performed using ^{1}H Nuclear Magnetic Resonance (NMR). The various polymers were dissolved to 50mg/mL in deuterated DMSO and evaluated in a Bruker AV 200MHz NMR spectrometer. Relevant peaks were integrated to determine the ratios of specific proton groups present in the material.

3.2.2 Molecular Weight

Molecular weight was calculated using the method outlined by Izunobi and Higginbotham (2011), with integral values taken from the same NMR spectra used to determine polymer composition. Molecular weight was calculated from Equation 1:

$$M_n = \sum(nx * M_{0x}) + M_e \qquad (1)$$

Where nx is the number of repeating units of each monomer in each chain, M_{0x} is the molecular weight of each monomer, and M_e is the molecular weight of the benzoyl peroxide end groups.

The number of repeating units of each monomer is calculated from Equation 2:

$$nx = \frac{ax*me*ne}{ae*mx} \qquad (2)$$

Where a is the area of the integral representing each peak, m is the number of protons represented by each peak, x denotes the specific monomer, and e represents the end group.

Molecular weight distributions were also characterized using gel permeation chromatography (GPC). Material was dissolved to approximately 5 mg/mL in THF and run through one of two GPC systems. The first system consisted of a Waters 515 HPLC pump, Waters 717plus Autosampler, three Waters Styragel columns, and a Waters 2414 refractive-index detector. The second system consisted of a Waters 2695 Separations Module equipped with three Polymer Labs PL gel individual pore-size columns, and a Waters 2414 refractive-index detector. Peaks were compared to polystyrene calibration curves to determine approximate molecular weights. It should be noted that polystyrene standards have slightly different solution properties than the target polymer, and therefore the calibration curve used may have given biased weights for the target polymer.

3.2.3 Lower Critical Solution Temperature

The lower critical solution temperature (LCST) of each of the polymers was determined by differential scanning calorimetry (DSC). Solutions of 300 mg/mL of polymer in phosphate-buffered saline (PBS) were assessed using a TA Instruments DSC 2910 Differential Scanning Calorimeter. Scanning occurred from 5^{o}C to 80^{o}C at a heating rate of 2^{o}C per minute. The locations of polymer phase transitions were determined using TA Instruments Thermal Analyst 2100 software.

3.2.4 Optical Transparency

Optical transparency of the materials was investigated using a Biotek Synergy 4 spectrometer at 37^{o}C. Samples dissolved to 300 mg/mL in PBS were plated on 96 well UV plates. 400 μL of sample was introduced to each well. After being inserted into the spectrometer, plates were allowed to sit for five minutes prior to reading absorbance values, in order to allow the temperature to equilibrate. Absorbance was read from 250 to 900 nm in 10 nm increments.

3.2.5 Viscosity

A TA Instruments ARES rheometer with 14 mm diameter plates was used to determine the dynamic viscosity of each polymer in solution. Samples were dissolved to approximately 300 mg/mL in PBS before undergoing viscosity measurements. A dynamic strain test was first performed to determine the linear viscoelastic region, where viscoelastic properties would be independent of imposed strain and so the relationship between viscoelastic properties and molecular structure could be more adequately evaluated. A dynamic frequency test was then performed within the limits of this linear viscoelastic region to determine how the viscosity changed with frequency of applied strain. The dynamic frequency test also provided information for evaluation of certain viscoelastic properties of the sample.

3.2.6 Refractive Index

Refractive index testing was performed using an Atago PAL pocket refractometer. Samples were dissolved to 300 mg/mL in PBS: 0.3 mL of sample was introduced onto the

detector. The apparatus was then placed in a 37°C oven for 5 minutes to allow the material to gel and refractive index readings taken immediately upon removal from the oven.

3.2.7 Cellular Compatibility

Cellular compatibility was assessed using retinal pigment epithelial (RPE) cells obtained from ATCC (Manassas, VA). RPE cells were cultured in Dulbecco's Modified Eagle Medium: Nutrient Mixture F-12, supplemented with 10% fetal bovine serum and 10 U/mL penicillin/streptomycin antibiotic. Cells were maintained at 37°C in a humidified 5% CO_2 environment. To determine cellular compatibility, cells were seeded at 3.5 x 10^4 cells per well onto 24-well plates in 0.3 μm pore size cell culture inserts and allowed to grow for 24 hours prior to exposure to polymer solutions. Polymers were sterilized using gamma irradiation and dissolved to 300 mg/mL in sterile PBS. The medium on top of the cells was replaced with polymer solution and allowed to incubate for 24 hours before being removed. Toxicity was then determined using standard MTT assay. After removal of polymer and cell culture medium, 500 μL of 0.5 mg/mL MTT solution in sterile PBS was introduced into each well and allowed to incubate for 4 hours. The solution was then aspirated and 600 μL dimethyl sulfoxide was added to each well to dissolve the crystals formed. This solution was then transferred in 200 μL aliquots to a 96-well plate and absorbance read at 570 nm.

4.0 Results and Discussion

4.1 Polymerization

Polymerization and subsequent purification resulted in polymer isolates of varying physical appearance. While most samples appeared as a fine white powder, some were more cohesive solids. Feed ratios were selected based on previous development of degradable transparent PNIPAAm gels. Polymers in solution exhibited characteristic LCST behavior upon heating to 37^{o}C, precipitating at low concentrations and forming viscous "gels" at higher concentrations (> ~250 mg/mL). The gel behavior of these materials above a critical concentration is thought to be attributable to polymer chain entanglements and the physical association of polymer precipitates (Jyeong, Kim and Bae 2012). A summary of the polymer characteristics is given in Table 1, while Figure 5 demonstrates the varying viscosity and transparency of the gels formed.

Table 1. Summary of polymer characteristics

Polymer feed ratio (Mw PEG/ NIPAAm:NAS:PEG)	Physical Appearance	Solution behavior at 37°C
475/ 88:0:12	Cohesive powder	Liquid/transparent
475/ 88:4:8	White powder	Stiff/translucent
475/ 92:0:8	White powder	Viscous/transparent
475/ 92:3:5	White powder	Viscous/transparent
475/ 88:6:6	White powder	Viscous/transparent
475/ 92:4:4	Cohesive powder	Stiff/opaque
475/ 88:2:10	White powder	Viscous/translucent
950/ 88:6:6	White powder	Viscous/transparent
950/ 92:0:8	White powder	Viscous/transparent
950/ 88:0:12	Cohesive solid	Liquid/transparent
1100/ 88:2:10	Cohesive solid	Liquid/transparent
1100/ 92:3:5	White powder	Liquid/transparent
1100/ 92:4:4	Cohesive powder	Viscous/translucent
1100/ 90:5:5	White powder	Viscous/transparent
950/ 92:1:7	Cohesive powder	Liquid/transparent
1100/ 88:4:8	Cohesive solid	Liquid/transparent

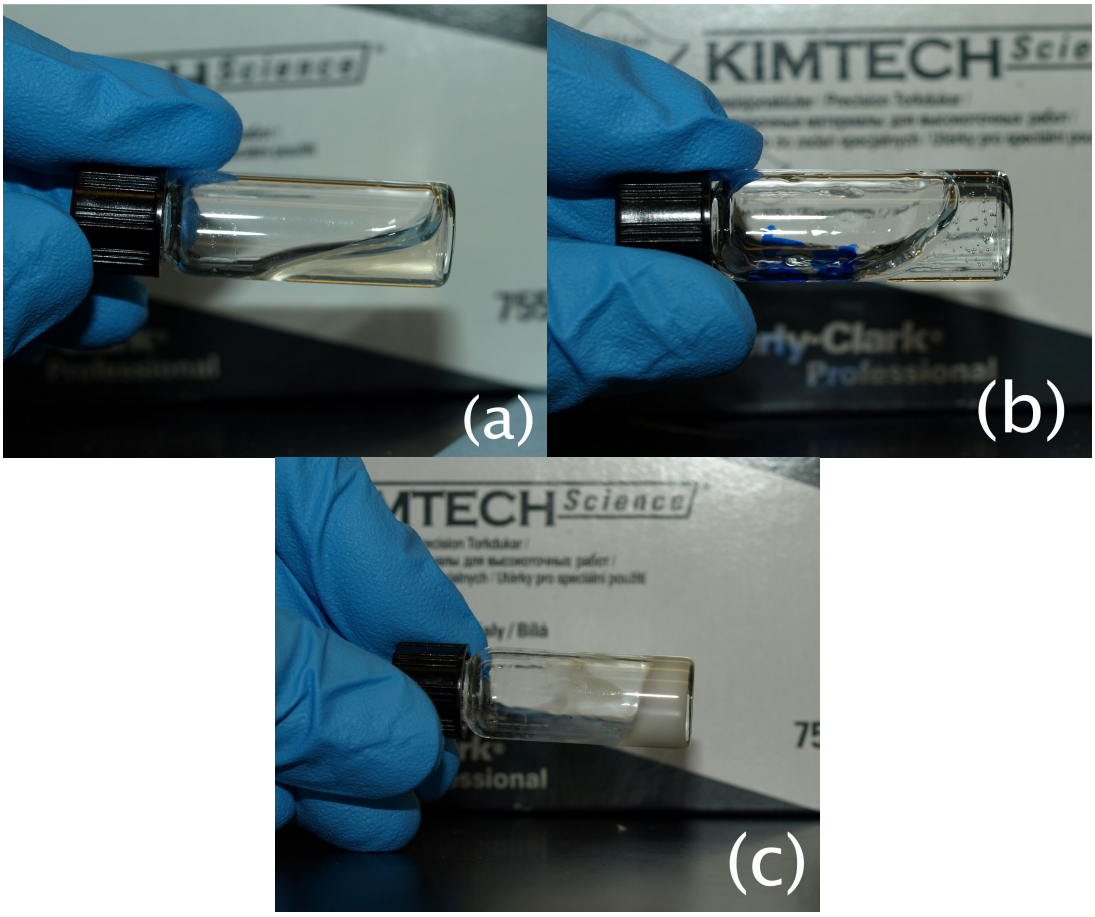

Figure 5. Varying gel behaviour of polymer solutions at 37°C (a) $PNNP_{475}$ 88:2:10 (b) $PNNP_{1100}$ 92:4:4 (c) $PNNP_{475}$ 92:4:4

4.2 Polymer Characterization

4.2.1 Polymer Composition

Through NMR testing, the ratio of initial reagents present in the final polymer was determined. A sample NMR spectrum with identification of relevant peaks is shown below in Figure 6. Results are summarized in Table 2 and Table 3.

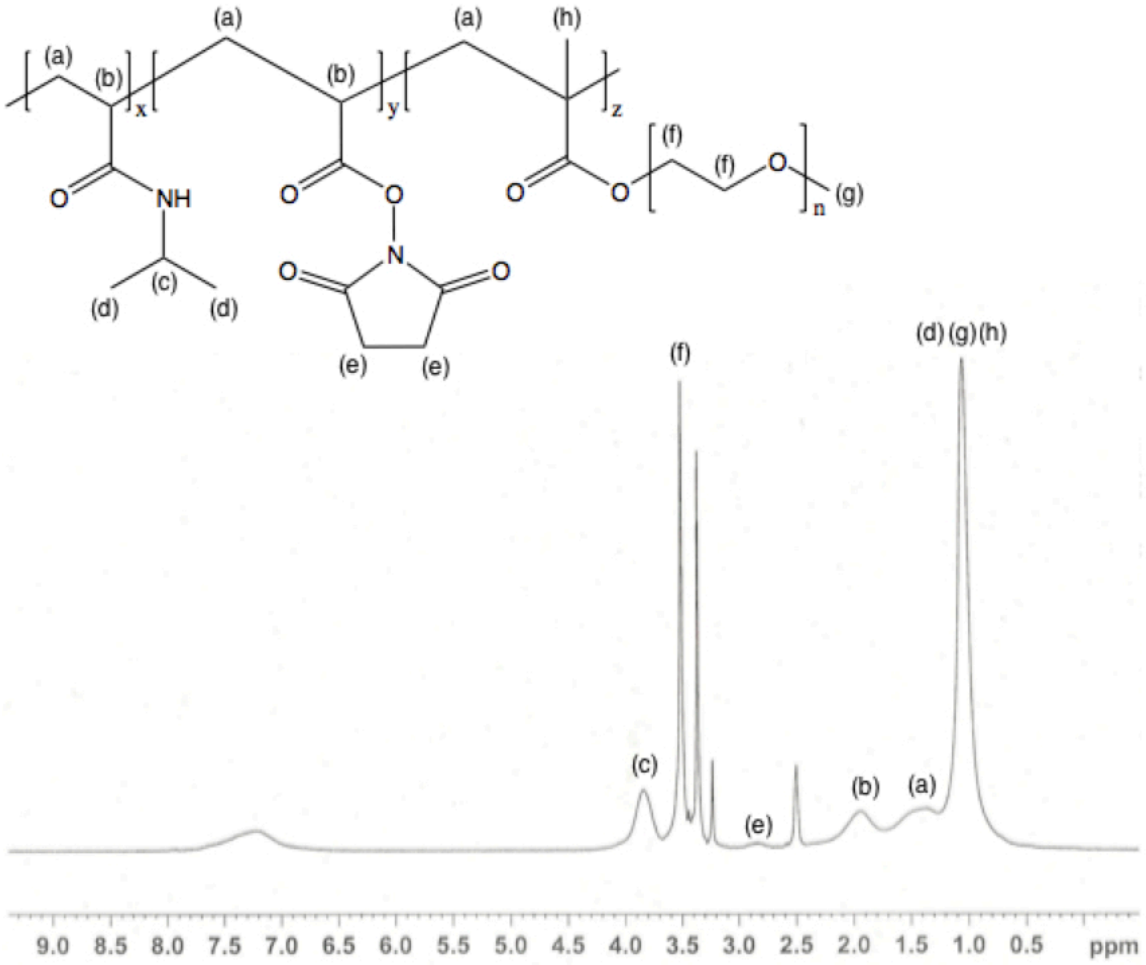

Figure 6. NMR Spectrum of PNNP

In most cases the side-chain ratio approximated the initial feed ratio; however, in cases where the feed ratio contained a lower mole percent of NIPAAm, the final polymer was more likely to contain a greater number of NIPAAm side-chains than was present in the initial feed. It was hypothesized that this was due to the higher reactivity of NIPAAm in the polymerization solution compared to the other monomers. Tables 2 and 3 show the initial feed concentrations and resulting polymer side-chain ratios.

Table 2. Polymer composition of $PNNP_{1100/950}$ as determined by NMR

Feed ratio (NIPAAm:NAS:PEG)	Polymer ratio as determined by NMR (NIPAAm:NAS:PEG)
92:4:4	93:4:3
92:3:5	93:3:4
92:1:7	92:1:7
92:0:8	93:0:7
90:5:5	92:4:4
88:6:6	90:5:5
88:4:8	89:4:7
88:2:10	92:1:7
88:0:12	92:0:8

Table 3. Polymer composition of $PNNP_{475}$ as determined by NMR

Feed ratio (NIPAAm:NAS:PEG)	Polymer ratio as determined by NMR (NIPAAm:NAS:PEG)
92:4:4	92:4:4
92:3:5	93:3:4
92:0:8	93:0:7
88:6:6	90:5:5
88:4:8	89:4:7
88:2:10	89:2:9
88:0:12	90:0:10

4.2.2 Molecular Weight

Molecular weight was also determined from NMR spectra. As the number of protons represented by the benzoyl peroxide end group peak is known to be 5 and an ideal linear polymer chain will contain 2 end groups, we can use Equation 2 to derive Equation 3:

$$nX = 10\ \frac{aX}{(ae*mX)} \qquad (3)$$

Using Equations 1 and 3, an estimate for the average molecular weight of each of the polymer formulations can then be derived. The results are shown below in Tables 4 and 5.

Table 4. Molecular weights of $PNNP_{950/1100}$ as determined by NMR

Feed ratio (NIPAAm:NAS:PEG)	Molecular weight calculated by end-group analysis (g/mol)
92:4:4	2406
92:3:5	2632
92:1:7	3619
92:0:8	3300
90:5:5	2770
88:6:6	2828
88:4:8	3630
88:2:10	4122
88:0:12	4177

Table 5. Molecular weights of $PNNP_{475}$ as determined by NMR

Feed ratio (NIPAAm:NAS:PEG)	Molecular weight calculated by end-group analysis (g/mol)
92:4:4	1923
92:3:5	1941
92:0:8	2302
88:6:6	2221
88:4:8	2444
88:2:10	2642
88:0:12	2761

These numbers seem quite low, especially when compared to the theoretical molecular weights of such polymer systems, as calculated by Equation 4 (Ganachaud, et al. 2000):

$$MW_{polymer} = \frac{[monomer]}{[initiator]} \times MW_{monomer} \times conversion \qquad (4)$$

Conversion is expected to be close to 1 for an ideal free-radical polymerization (Tefera, et al. 1994). According to Equation 4, the molecular weights of these polymers are expected to be on the order of 12000 g/mol. This discrepancy is likely due to the challenges associated with using NMR to determine molecular weights. It has been well established that this method of molecular weight determination does not provide accurate estimations for every polymer system (Procházka and Kratochvíl 1987). It is possible that the polymer chains could adopt a conformation in solution that results in internal side chains

being "hidden" and not influencing the NMR results. Low molecular weights could also be due to the uncontrolled nature of the polymerization. While polymerization events such as disproportionation, scission or backbiting of the polymer chain were not expected to be significant at the low temperatures used in the reaction, the possibility of these events occurring still exists and would result in chains of lower molecular weight (Asua, et al. 2004). Additionally, it is possible that the initiator is attacking side chain groups as well as terminal vinyl groups, resulting in branched polymer chains that contain more than two benzoyl peroxide groups.

Despite the low molecular weight estimates derived by end-group analysis, the molecular weights of these polymers can still be compared to one another in order to assess whether trends existed. The molecular weight is seen to vary depending on the molecular weight of the PEG sidechains as expected as well as with the ratio of each monomer present in the initial feed. This result is to be expected due to the difference in molecular weights of the monomers as well as the different lengths of PEG used.

Molecular weight can also be determined by other means such as gel permeation chromatography (GPC) and mass spectrometry. Unfortunately, numerous issues were encountered during attempts to characterize the polymer using GPC. Because GPC relies on calibration with polymers of narrowly dispersed molecular weights, the results obtained from this method may not be accurate if the polymers used in calibration differ significantly from the polymer being characterized. In this case, the GPC columns used were calibrated with polystyrene standards, which contain many structural differences from the polymers studied, especially if some branching has occured. Additionally, the

type of column used will affect the residence time of the polymer and different columns may give different molecular weight estimates. While attempting to characterize our polymers through GPC, two separate columns were used which gave vastly different estimates of molecular weight. The first column gave results on the order of 20-30 kDa while the second gave results on the order of 5-10 kDa. This was attributed to differences in flow rate as well as column size and packing, as the mobile phase in each column was the same. However, these differences made it difficult to determine accurately the molecular weights of the polymers prepared. GPC results are summarized in Table 6.

Table 6. Molecular weights and polydispersities of polymer samples as determined by GPC

Monomer ratio (NIPAAm:NAS:PEG)	**(Styragel GPC)**			**(Adronov GPC)**		
	Mn (g/mol)	**Mw (g/mol)**	**PD**	**Mn (g/mol)**	**Mw (g/mol)**	**PD**
1100 92:3:5	27024	60143	2.226	4873	8356	1.715
1100 88:4:8	21182	42554	2.331	2802	3217	1.148
1100 92:4:4	28360	42554	2.009	3147	3818	1.213
1100 90:5:5	-	-	-	3909	5053	1.293
475 88:2:10	-	-	-	3980	5226	1.313
1100 92:1:7	-	-	-	3839	4794	1.249
950 92:0:8	-	-	-	3183	5137	1.614
475 92:0:8	-	-	-	11396	21694	1.904
475 88:0:12	-	-	-	10438	19080	1.828
475 92:4:4	-	-	-	9723	19532	2.009

4.2.3 Lower Critical Solution Temperature

Thermal analysis of the polymers was carried out using differential scanning calorimetry (DSC). DSC was chosen over more prevalent tests such as turbidity measures due to the expected transparency of the polymer systems. As expected, based on the presence of the NIPAAm in the samples, most polymer samples displayed a characteristic exothermic peak near 32^{o}C, indicating the presence of a LCST. Some samples also displayed an endothermic peak at a lower temperature, which could indicate an alteration in the LCST as a result of the polymerization of the NIPAAm with other more hydrophobic species. A summary of the onset of the LCST peaks is displayed in Tables 7 and 8 below.

Table 7. LCST values for $PNNP_{1100/950}$ as determined by DSC. Error represents standard deviation

Feed ratio (NIPAAm:NAS:PEG)	**LCST (^{o}C)**
92:4:4	33.92 ± 5.63
92:3:5	none
92:1:7	none
92:0:8	none
90:5:5	34.46 ± 0.57
88:6:6	none
88:4:8	none
88:2:10	none
88:0:12	none

Table 8. LCST values for $PNNP_{475}$ as determined by DSC

Feed ratio (NIPAAm:NAS:PEG)	LCST (^{o}C)
92:4:4	28.52 ± 0.47
92:3:5	30.60 ± 0.28
92:0:8	35.43 ± 0.12
88:6:6	30.77 ± 0.24
88:4:8	34.04 ± 0.18
88:2:10	38.69 ± 0.51
88:0:12	40.05 ± 0.11

These results indicate a slight dependence of LCST on the feed ratio of the various monomers. The results obtained for polymers using higher molecular weight PEG show a significant difference from those using the same monomer ratios with a lower molecular weight PEG, although there are too few results to draw any general conclusions with confidence. However, the difficulty encountered in producing results may be indicative of a trend in itself; the LCST of these polymers may be so high that they lie outside the range of the DSC performed. These results may also be correlated to the properties of the materials in Table 1; most of the polymers that were difficult to obtain DSC data for were also observed to remain liquid at 37^{o}C. Further work could involve optimization of the LCST through manipulation of PEG chain length and monomer ratios.

Due to the nature of DSC it was sometimes difficult to obtain repeatable results. Because of the small sample used for each run and the broad molecular weight distribution observed, it is possible that differences in chain length and polymer composition, as well as solution mixing, could have contributed to the deviations encountered in some cases. Additionally, because of the length of time required to repeat all the DSC runs and the fact that samples were prepared ahead of time, it is possible that the solution profile may have been altered by redistribution of the solute, or some degradation of the material in solution may have occurred. Longer-term stability studies could be useful in assessing the contribution of these effects, should they exist, to the LCST and other properties of the materials.

It may also be possible to determine the LCST of a solution by temperature-controlled viscosity studies. While this was initially investigated as part of the rheometric studies performed on these polymers, the forced-air nature of the temperature control in the rheometer meant that evaporative effects rendered the results of such studies unreliable. Future work could look into alternative methods, such as light scattering, to determine LCST.

4.2.4 Optical Transparency

Light transmittance through the polymer solutions was determined using a BioTek spectrometer. As shown in the figures below, all but one of the polymer gels allowed transmittance between 80 and 90 percent in the visible spectrum.

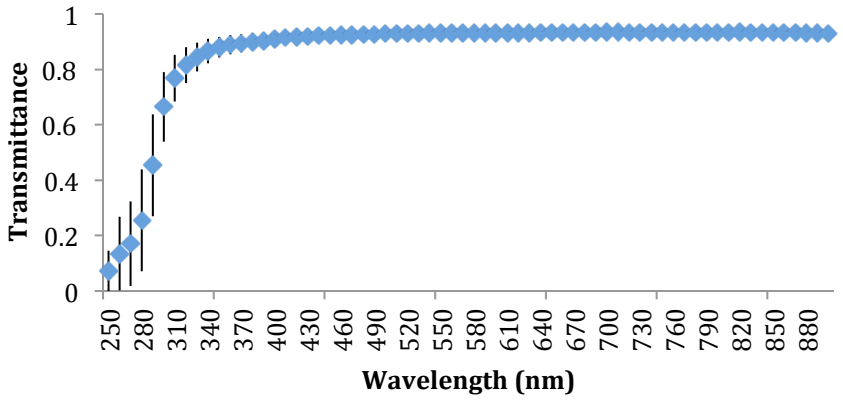

Figure 7. Transmittance of $PNNP_{1100}$ 88:2:10 (300 mg/mL in PBS) at 37°C. Error bars represent standard deviation

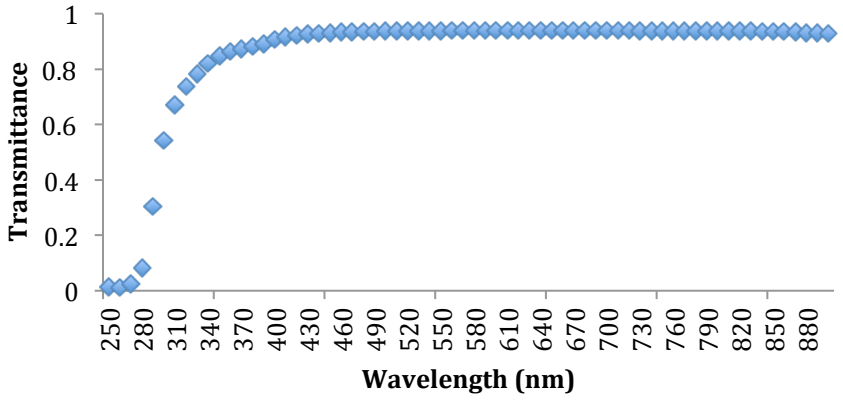

Figure 8. Transmittance of $PNNP_{1100}$ 90:5:5 (300 mg/mL in PBS) at 37°C. Error bars represent standard deviation

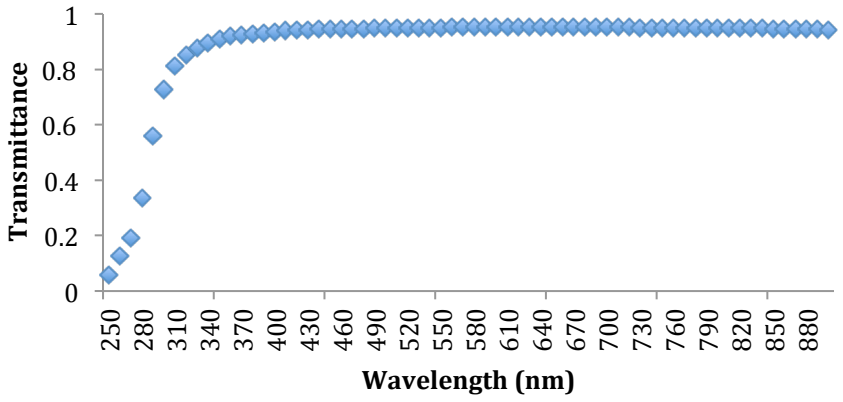

Figure 9. Transmittance of $PNNP_{1100}$ 92:1:7 (300 mg/mL in PBS) at 37°C. Error bars represent standard deviation

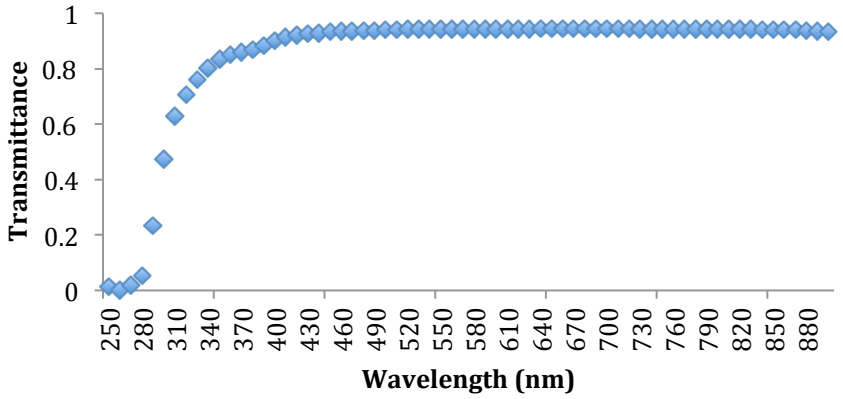

Figure 10. Transmittance of $PNNP_{1100}$ 88:4:8 (300 mg/mL in PBS) at 37°C. Error bars represent standard deviation

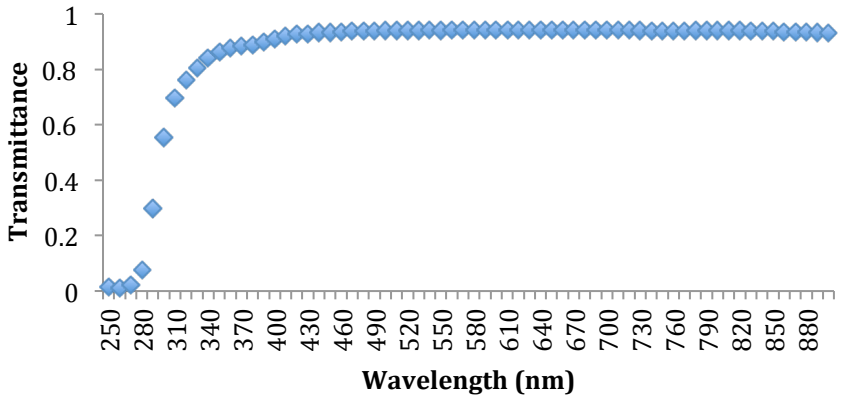

Figure 11. Transmittance of $PNNP_{1100}$ 92:3:5 (300 mg/mL in PBS) at 37°C. Error bars represent standard deviation

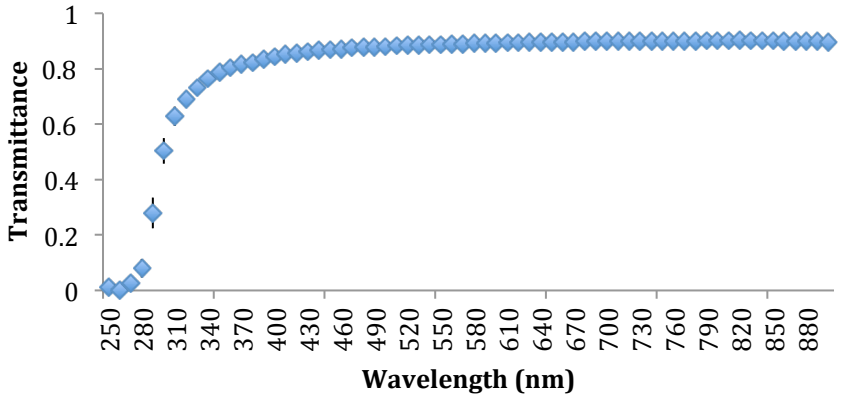

Figure 12. Transmittance of $PNNP_{1100}$ 92:4:4 (300 mg/mL in PBS) at 37°C. Error bars represent standard deviation

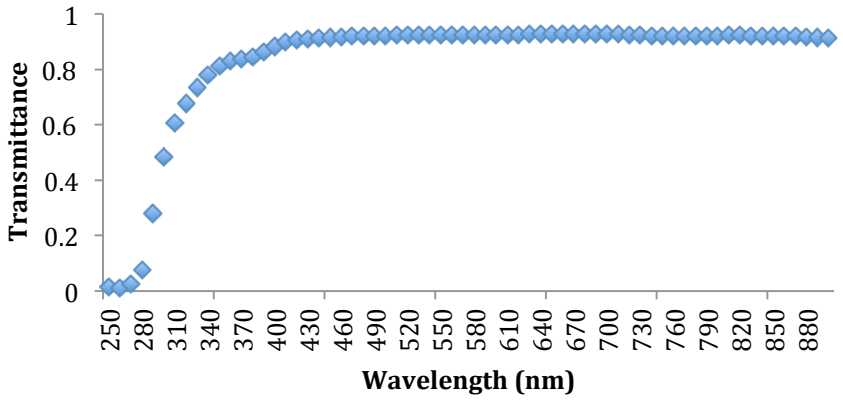

Figure 13. Transmittance for $PNNP_{950}$ 88:6:6 (300 mg/mL in PBS) at 37°C. Error bars represent standard deviation

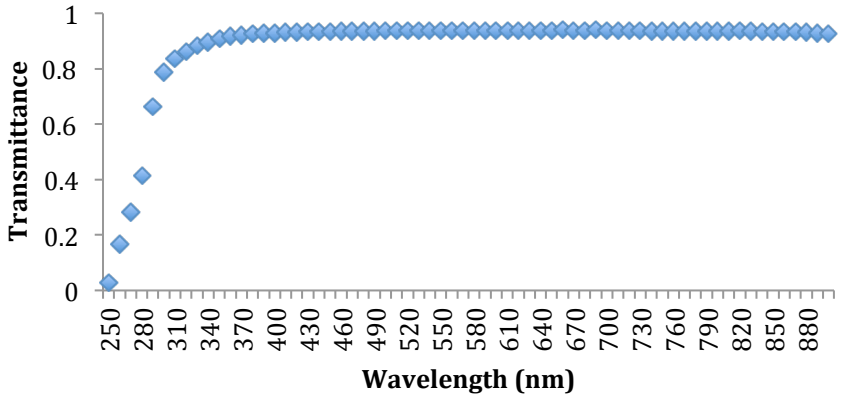

Figure 14. Transmittance for $PNNP_{950}$ 92:0:8 (300 mg/mL in PBS) at 37°C. Error bars represent standard deviation

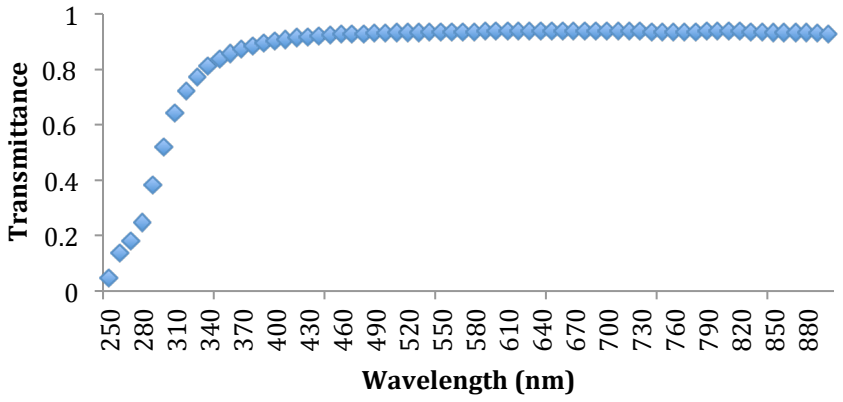

Figure 15. Transmittance for $PNNP_{950}$ 88:0:12 (300 mg/mL in PBS) at 37°C. Error bars represent standard deviation

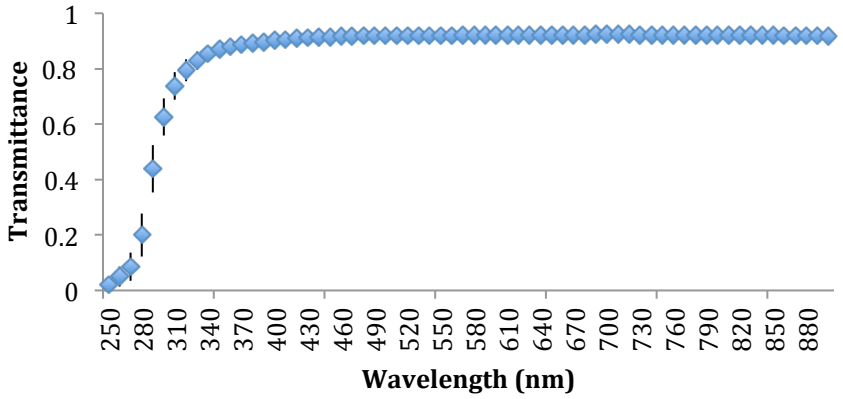

Figure 16. Transmittance of $PNNP_{475}$ 88:2:10 (300 mg/mL in PBS) at 37°C. Error bars represent standard deviation

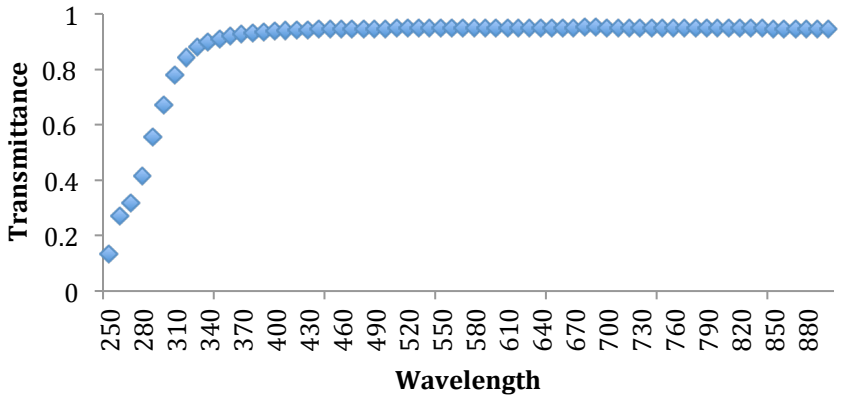

Figure 17. Transmittance of $PNNP_{475}$ 88:0:12 (300 mg/mL in PBS) at 37°C. Error bars represent standard deviation

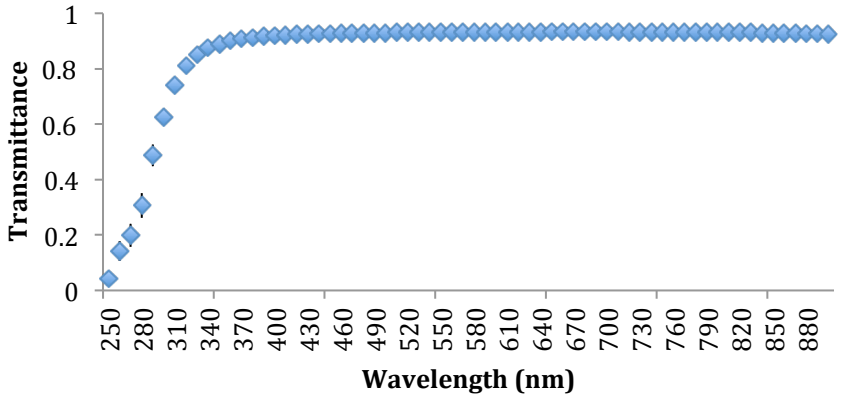

Figure 18. Transmittance of $PNNP_{475}$ 92:0:8 (300 mg/mL in PBS) at 37°C. Error bars represent standard deviation

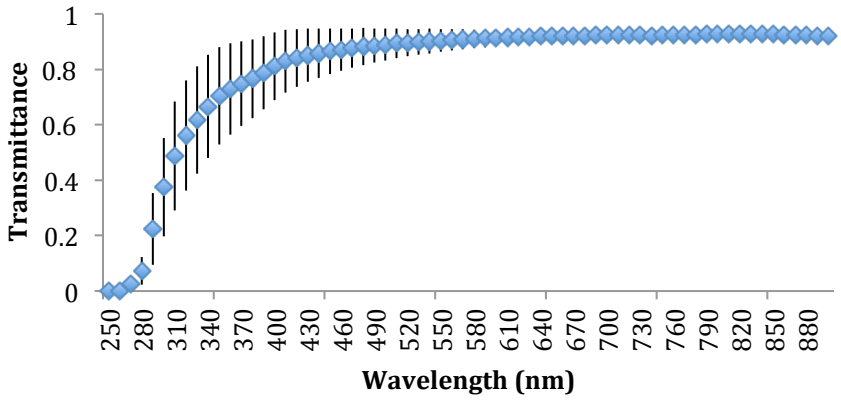

Figure 19. Transmittance of $PNNP_{475}$ 88:6:6 (300 mg/mL in PBS) at 37°C. Error bars represent standard deviation

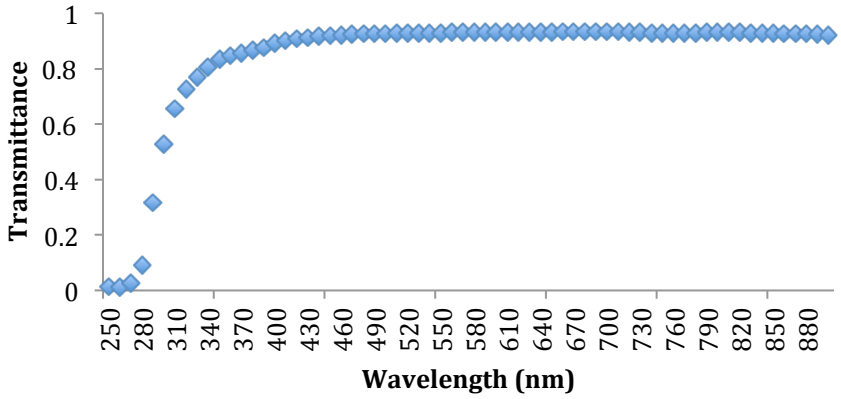

Figure 20. Transmittance of $PNNP_{475}$ 88:4:8 (300 mg/mL in PBS) at 37°C. Error bars represent standard deviation

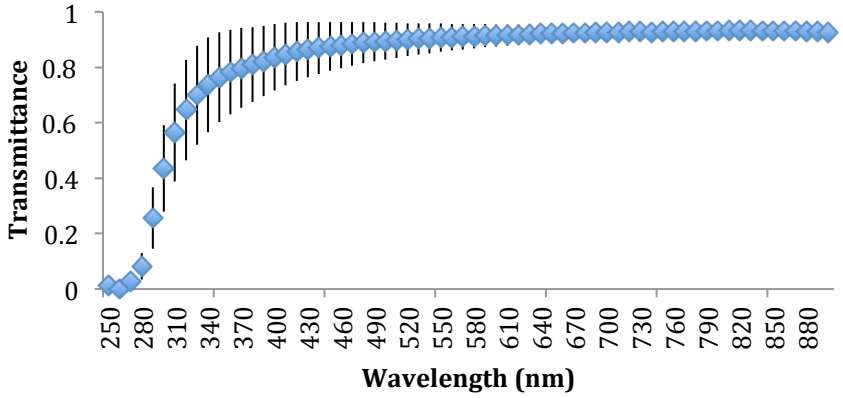

Figure 21. Transmittance of $PNNP_{475}$ 92:3:5 (300 mg/mL in PBS) at 37°C. Error bars represent standard deviation

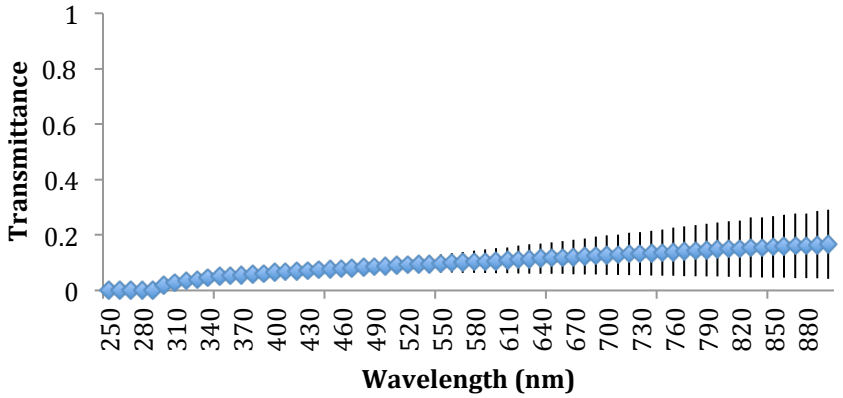

Figure 22. Transmittance of $PNNP_{475}$ 92:4:4 (300 mg/mL in PBS) at 37°C. Error bars represent standard deviation

When we compare these values to the transmittance of the native vitreous (Boettner and Wolter 1962), we see that in most cases the polymer gels provide adequate transmissibility for visible light.

The optical transparency of these materials can be loosely associated with both the molecular weight and the amount of PEG present in the material. However, these effects

are not especially strong except in the case of the 475 kDa molecular weight PEG with a NIPAAM:NAS:PEG ratio of 92:4:4, where lower transparency was observed. The reason for the greatly decreased transparency of this particular sample is unclear. It is possible that it is due to the confluence of the factors investigated, as it contains a lower number of PEG side chains as well as a lower molecular weight of PEG. This polymer sample also displayed the lowest LCST; previous studies have shown that a cloud point may be present in NIPAAm copolymers, where turbidity and mechanical strength greatly increase at a temperature above the LCST. It has been hypothesized that this effect is due to incomplete local self-association of polymer chains within the bulk of the solution (Fitzpatrick 2012). If these polymers also display such an effect, it could be possible that the cloud point of this polymer is the only one to fall below 37^{o}C. Turbidity studies should be performed to determine if this is the case. If we exclude the most drastic case, it appears that transparency varies significantly only with the amount of PEG present in the material; this may be because the difference in PEG chain length is not sufficient to change the optical properties.

4.2.5 Viscosity

Viscosity of the polymer solutions studied was assessed using an ARES rheometer with temperature controlled to 37°C. Both variable strain and variable frequency tests were performed, with parameters for the variable frequency tests chosen by selecting strain values near the upper limit of the linear viscoelastic region. In some cases the linear viscoelastic region was difficult to identify; this could be attributed to the incomplete association of molecules in solution near the LCST. Charts showing the changes in dynamic moduli of the material are shown below.

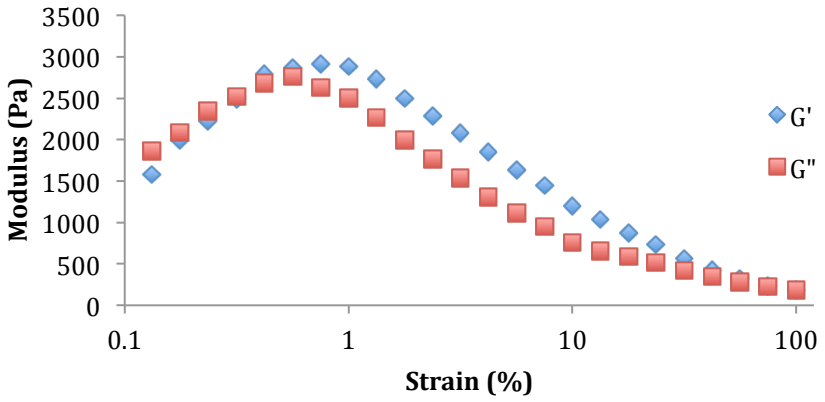

Figure 23. Dynamic strain curve for $PNNP_{1100}$ 88:4:8 (300 mg/mL) at 37°C. Error bars represent standard deviation

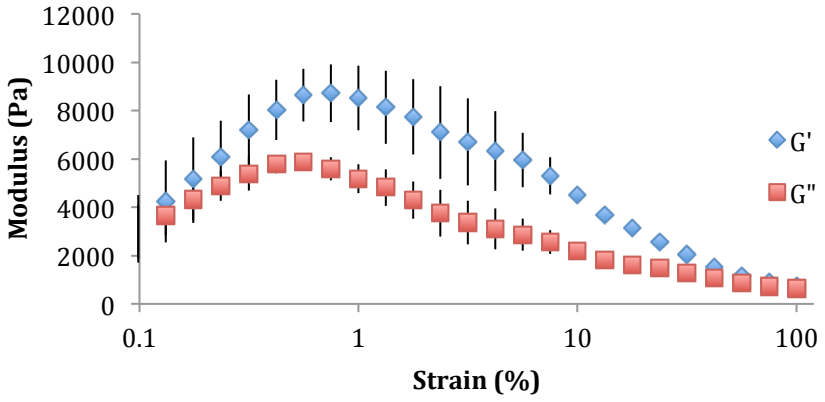

Figure 24. Dynamic strain curve for $PNNP_{1100}$ 92:1:7 (300 mg/mL in PBS) at 37°C. Error bars represent standard deviation

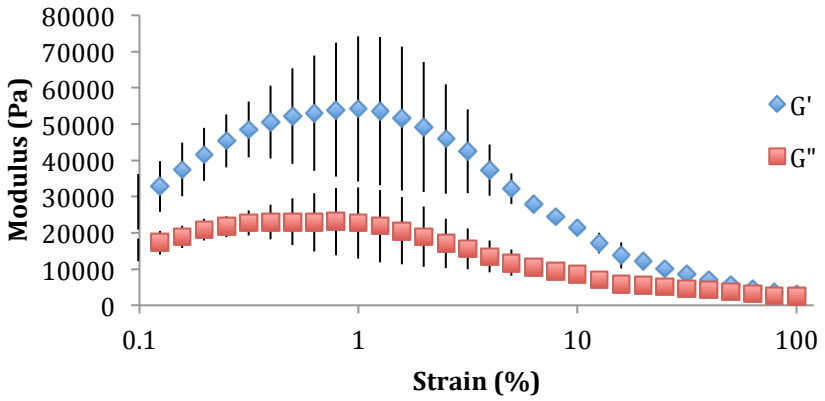

Figure 25. Dynamic strain curve for $PNNP_{1100}$ 90:5:5 (300 mg/mL in PBS) at 37°C. Error bars represent standard deviation

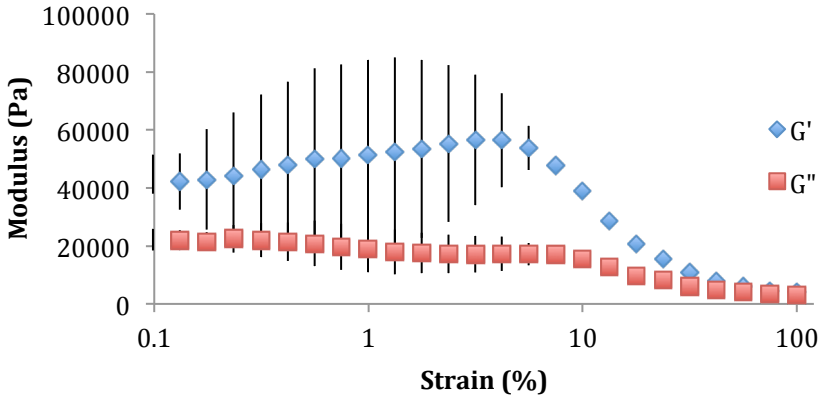

Figure 26. Dynamic strain curve for $PNNP_{1100}$ 92:4:4 (300 mg/mL in PBS) at 37°C. Error bars represent standard deviation

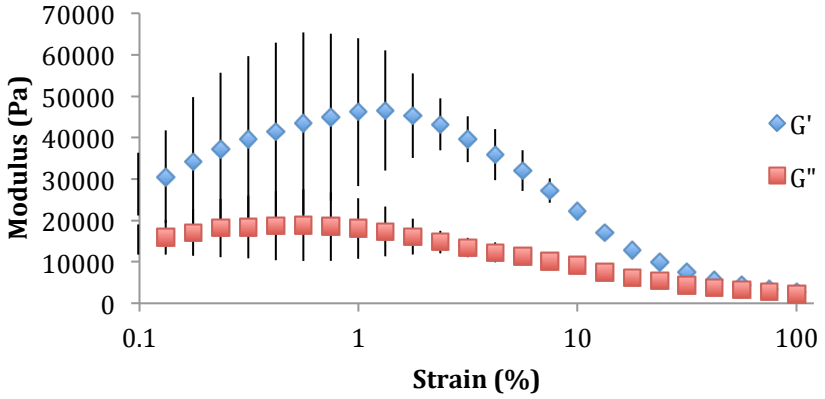

Figure 27. Dynamic strain curve for $PNNP_{1100}$ 92:3:5 (300 mg/mL in PBS) at 37°C. Error bars represent standard deviation

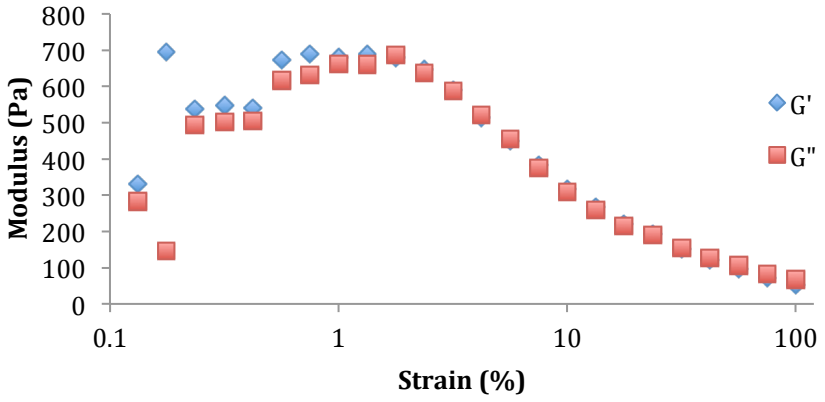

Figure 28. Dynamic strain curve for $PNNP_{1100}$ 88:2:10 (300 mg/mL in PBS) at 37°C. Error bars represent standard deviation

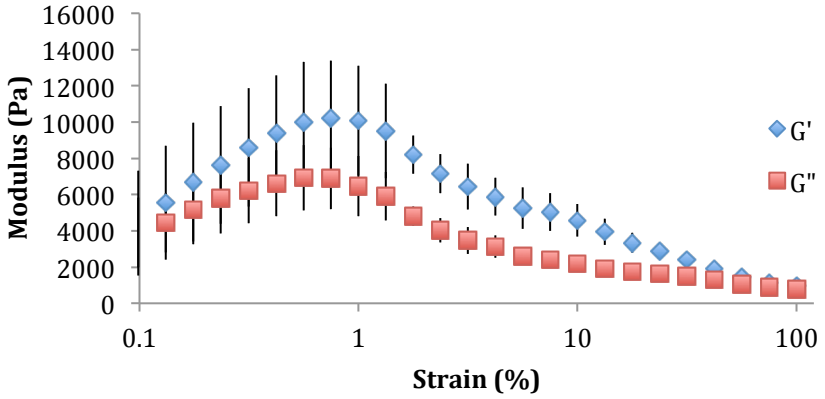

Figure 29. Dynamic strain curve for $PNNP_{950}$ 92:0:8 (300 mg/mL in PBS) at 37°C. Error bars represent standard deviation

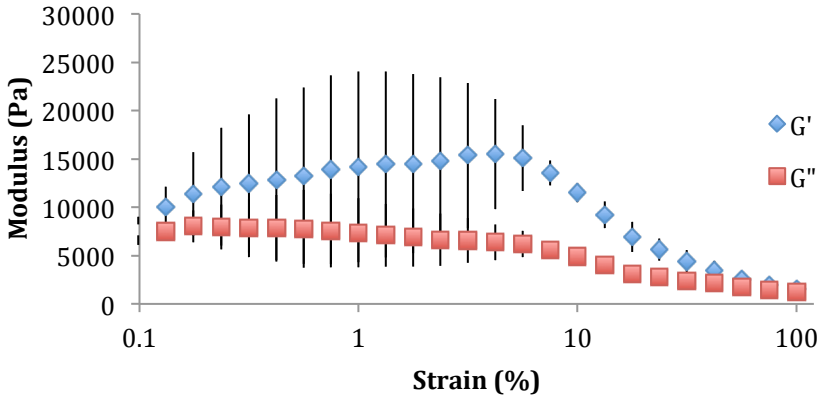

Figure 30. Dynamic strain curve for $PNNP_{950}$ 88:6:6 (300 mg/mL in PBS) at 37°C. Error bars represent standard deviation

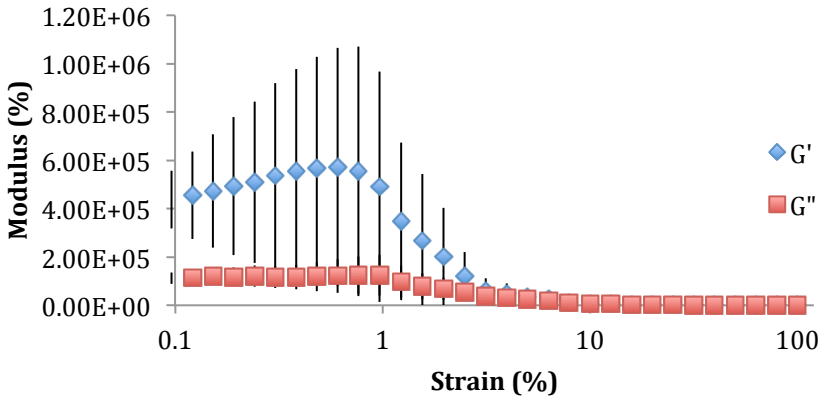

Figure 31. Dynamic strain curve for $PNNP_{475}$ 92:4:4 (300 mg/mL in PBS) at 37°C. Error bars represent standard deviation

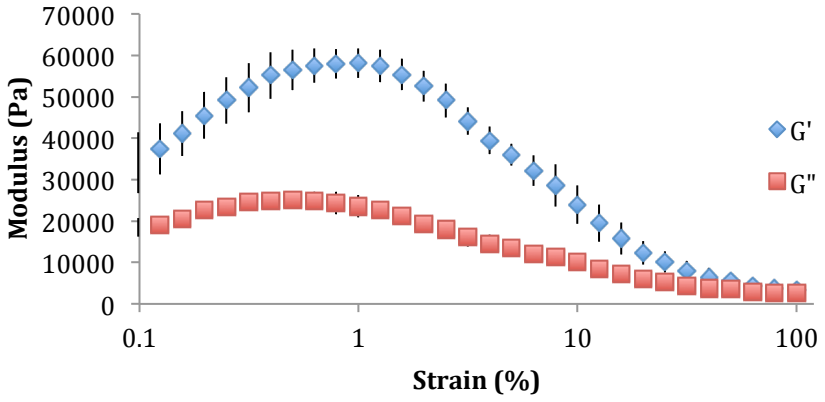

Figure 32. Dynamic strain curve for $PNNP_{475}$ 88:2:10 (300 mg/mL in PBS) at 37°C. Error bars represent standard deviation

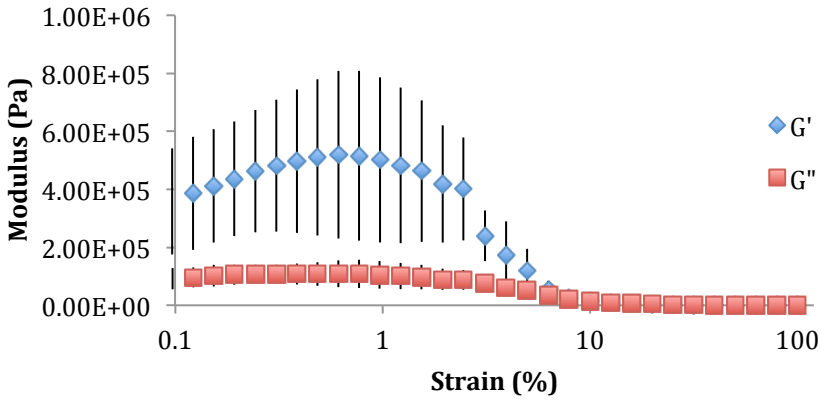

Figure 33. Dynamic strain curve for $PNNP_{475}$ 88:6:6 (300 mg/mL in PBS) at 37°C. Error bars represent standard deviation

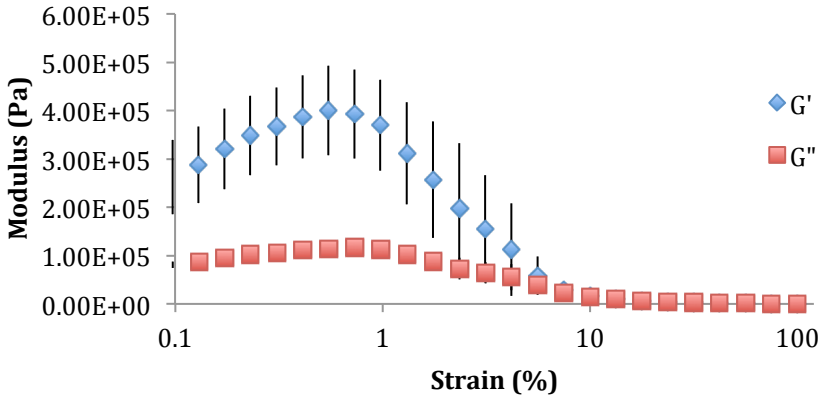

Figure 34. Dynamic strain curve for $PNNP_{475}$ 92:3:5 (300 mg/mL in PBS) at 37°C. Error bars represent standard deviation

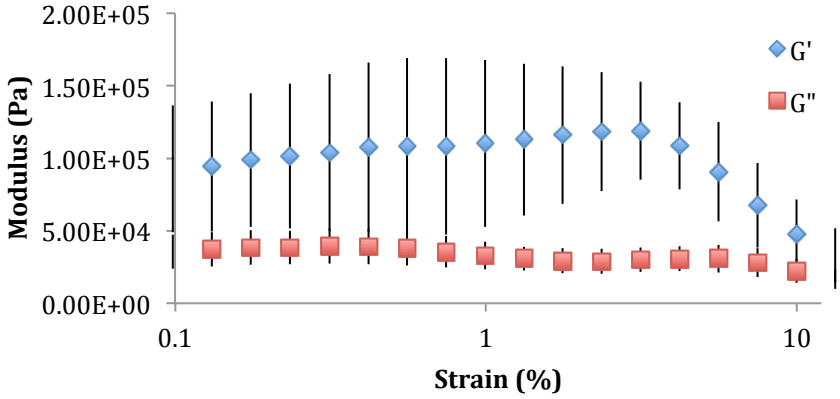

Figure 35. Dynamic strain curve for $PNNP_{475}$ 92:0:8 (300 mg/mL in PBS) at 37°C. Error bars represent standard deviation

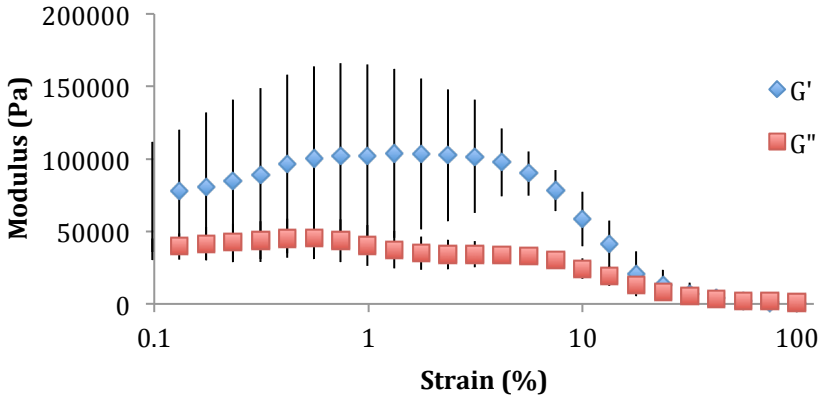

Figure 36. Dynamic strain curve for $PNNP_{475}$ 88:4:8 (300 mg/mL in PBS) at 37°C. Error bars represent standard deviation

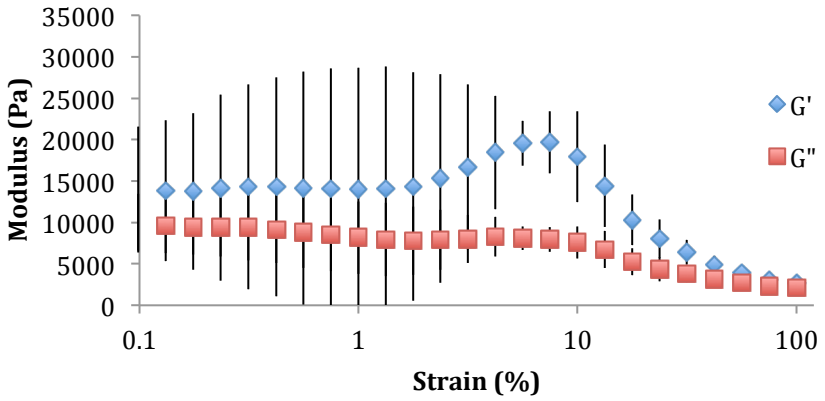

Figure 37. Dynamic strain curve for $PNNP_{475}$ 88:0:12 (300 mg/mL in PBS) at 37°C. Error bars represent standard deviation

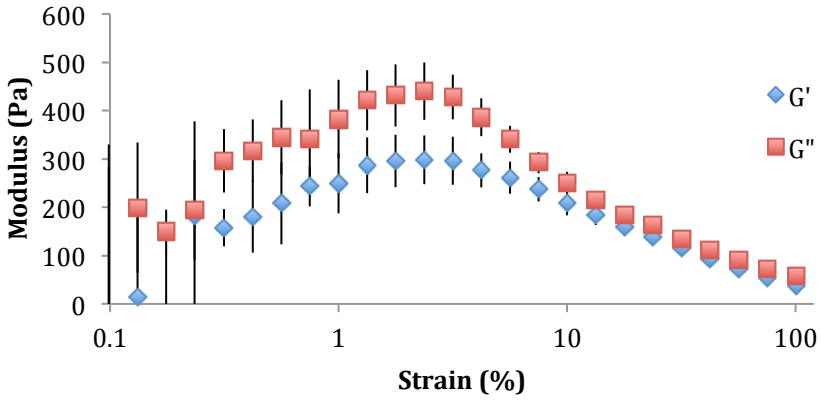

Figure 38. Dynamic strain curve for $PNNP_{950}$ 88:0:12 (300 mg/mL in PBS) at 37°C. Error bars represent standard deviation

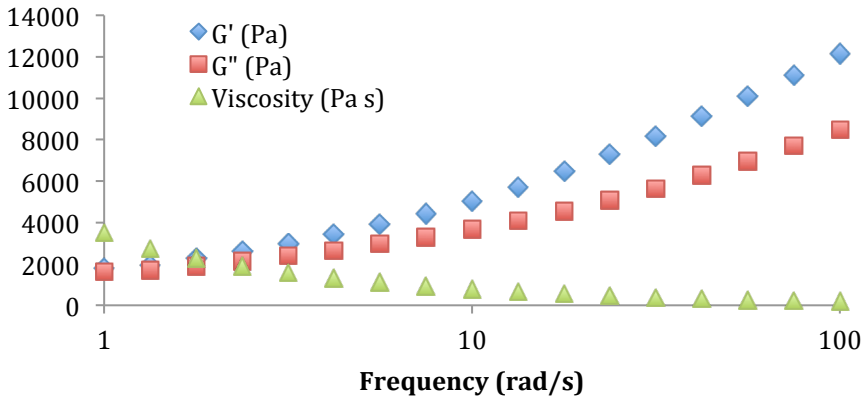

Figure 39. Dynamic frequency curve for $PNNP_{475}$ 88:0:12 (300 mg/mL in PBS) at 37°C

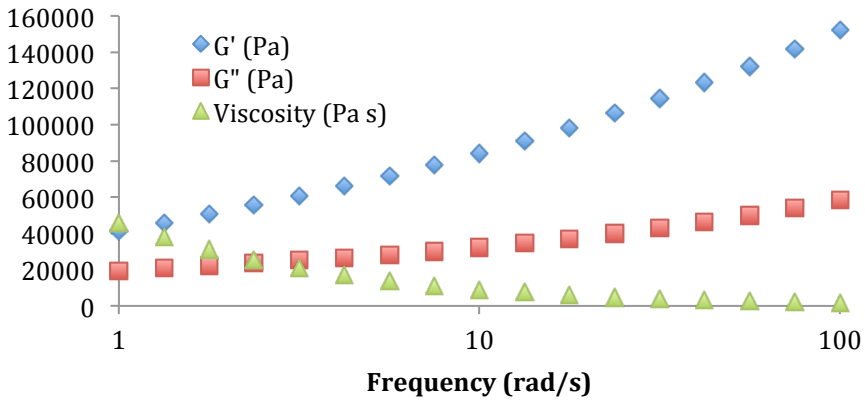

Figure 40. Dynamic frequency curve for $PNNP_{475}$ 88:4:8 (300 mg/mL in PBS) at 37°C

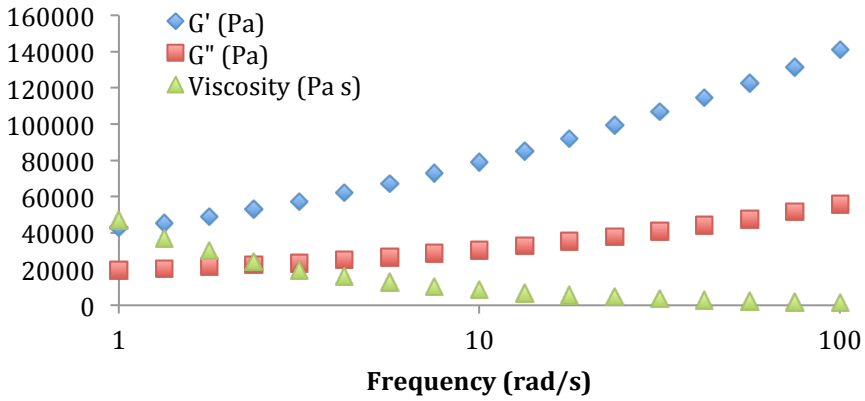

Figure 41. Dynamic frequency curve for $PNNP_{475}$ 92:0:8 (300 mg/mL in PBS) at 37°C

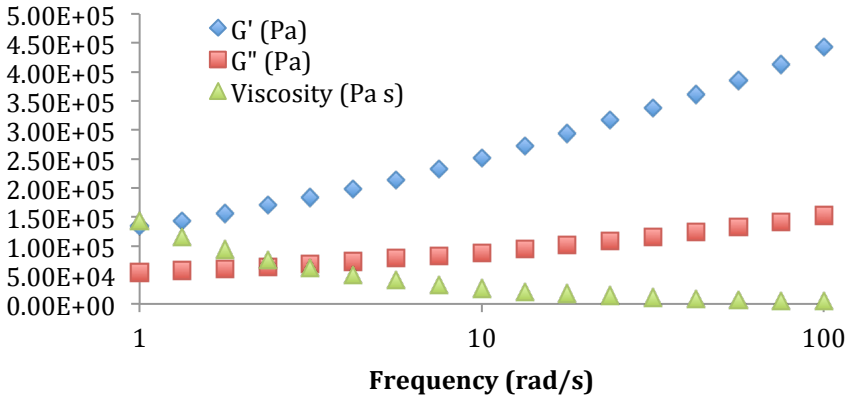

Figure 42. Dynamic frequency curve for $PNNP_{475}$ 92:3:5 (300 mg/mL in PBS) at 37°C

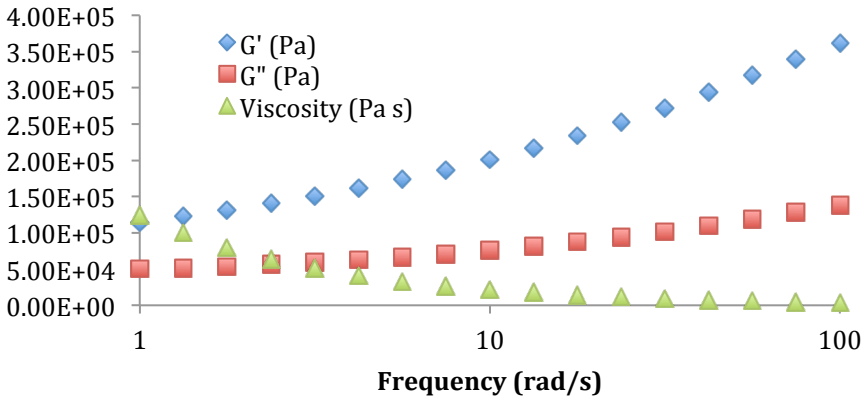

Figure 43. Dynamic frequency curve for $PNNP_{475}$ 88:6:6 (300 mg/mL in PBS) at 37°C

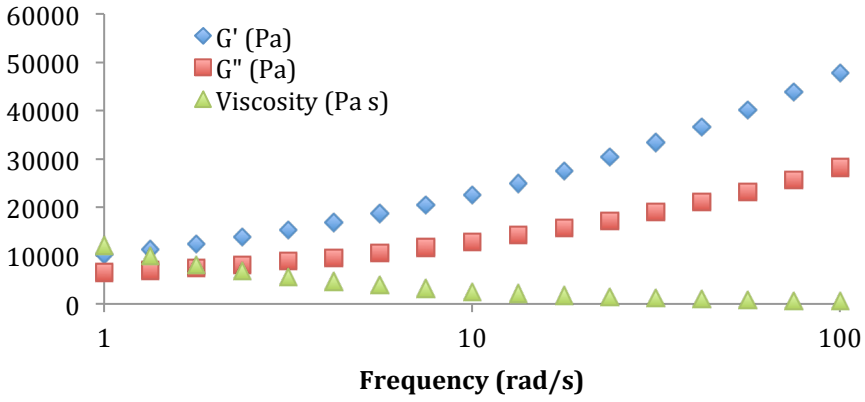

Figure 44. Dynamic frequency curve for $PNNP_{475}$ 88:2:10 (300 mg/mL in PBS) at 37°C

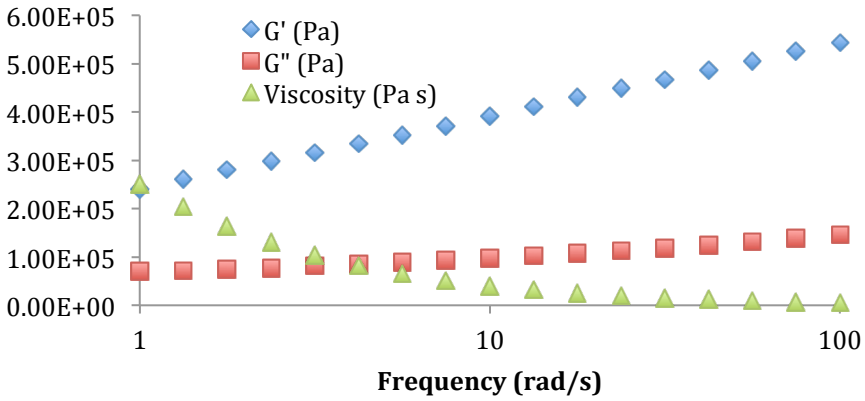

Figure 45. Dynamic frequency curve for $PNNP_{475}$ 92:4:4 (300 mg/mL in PBS) at 37°C

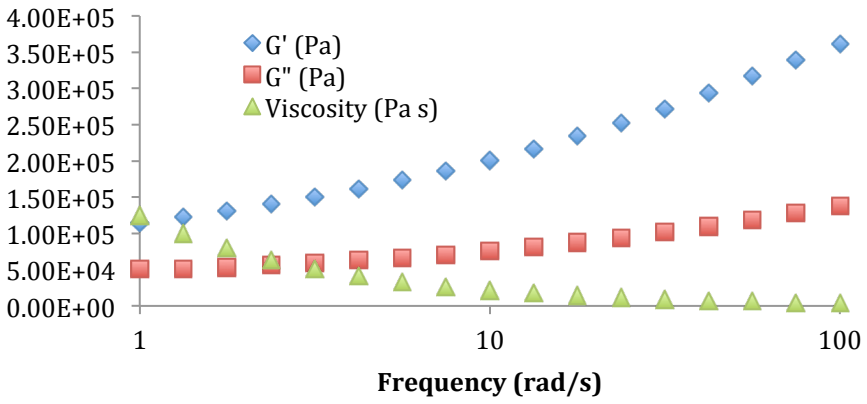

Figure 46. Dynamic frequency curve for $PNNP_{950}$ 88:6:6 (300 mg/mL in PBS) at 37°C

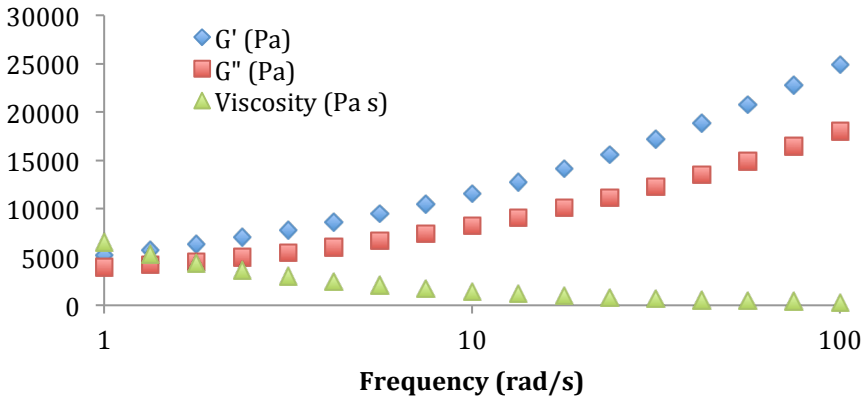

Figure 47. Dynamic frequency curve for $PNNP_{950}$ 92:0:8 (300 mg/mL in PBS) at 37°C

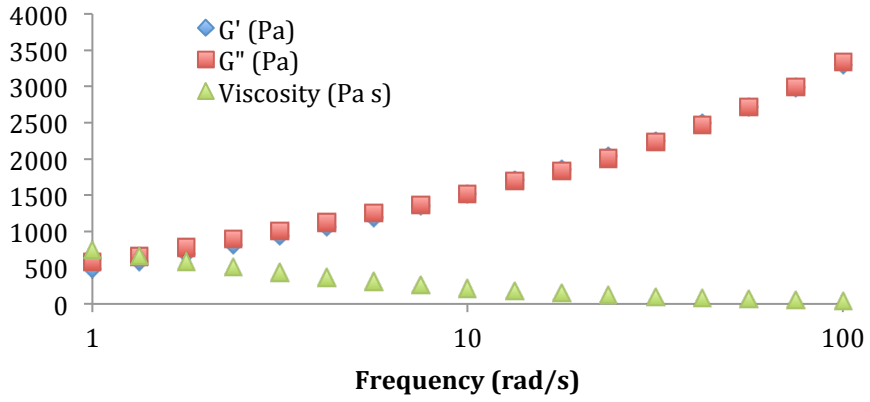

Figure 48. Dynamic frequency curve for $PNNP_{1100}$ 88:2:10 (300 mg/mL in PBS) at 37°C

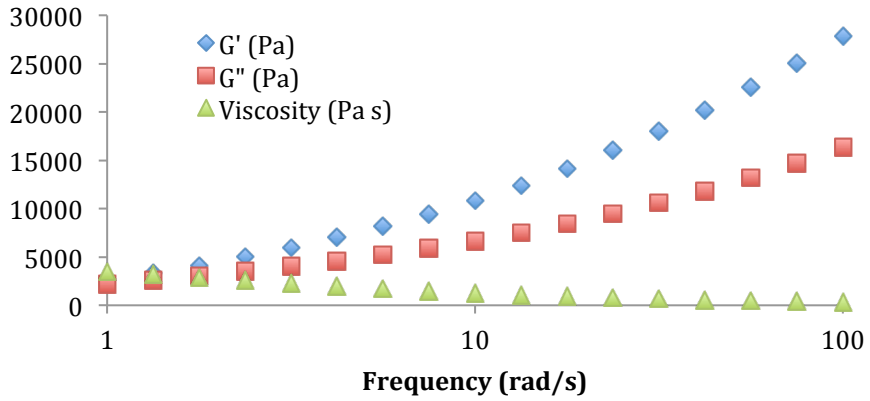

Figure 49. Dynamic frequency curve for $PNNP_{1100}$ 92:3:5 (300 mg/mL in PBS) at 37°C

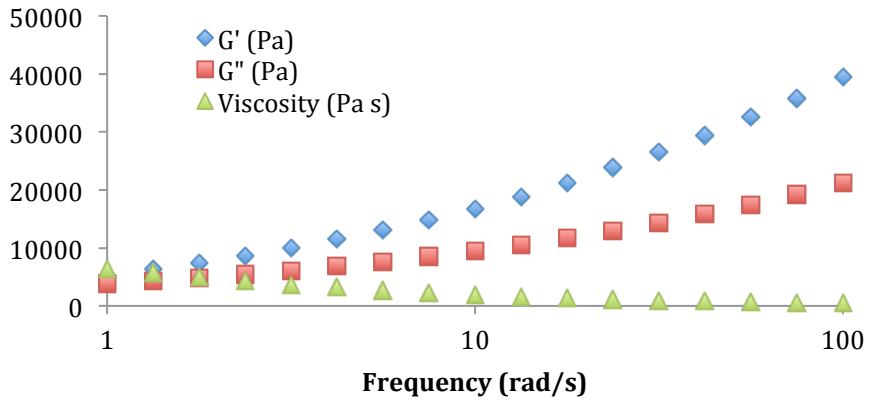

Figure 50. Dynamic frequency curve for $PNNP_{1100}$ 92:4:4 (300 mg/mL in PBS) at 37°C

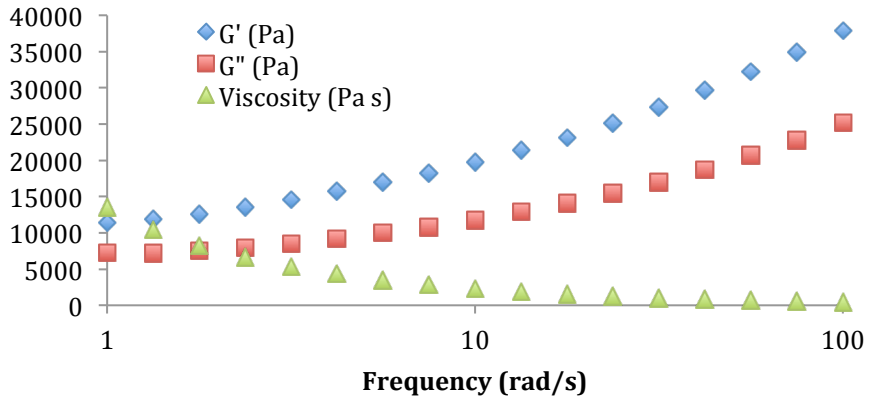

Figure 51. Dynamic frequency curve for $PNNP_{1100}$ 90:5:5 (300 mg/mL in PBS) at 37°C

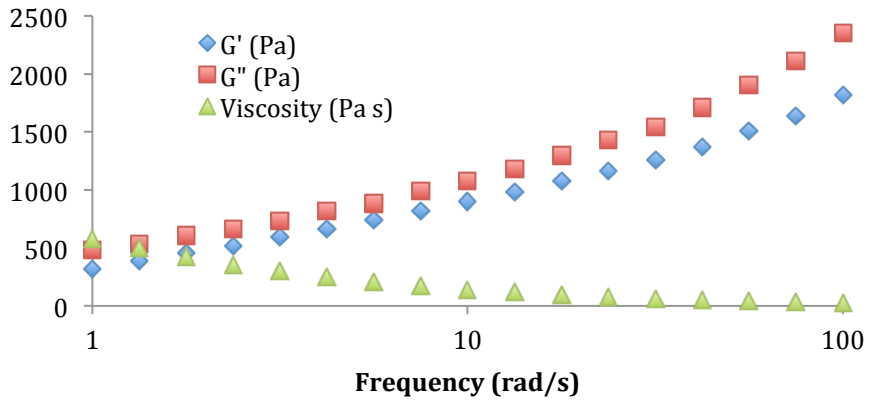

Figure 52. Dynamic frequency curve for $PNNP_{950}$ 88:0:12 (300 mg/mL in PBS) at 37°C

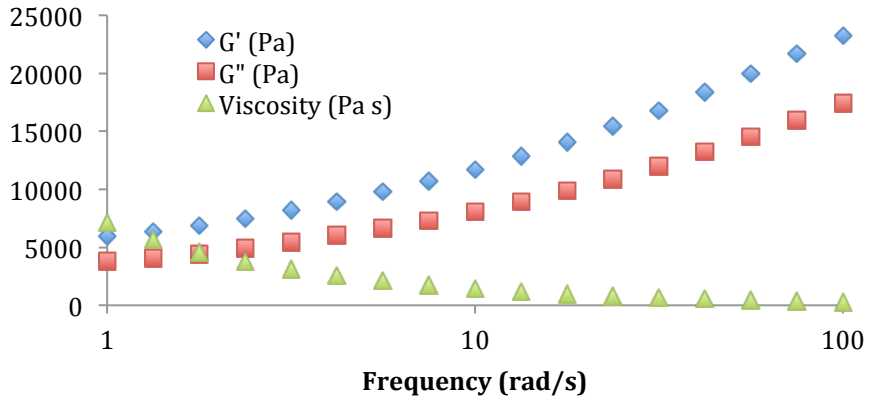

Figure 53. Dynamic frequency curve for $PNNP_{1100}$ 92:1:7 (300 mg/mL in PBS) at 37°C

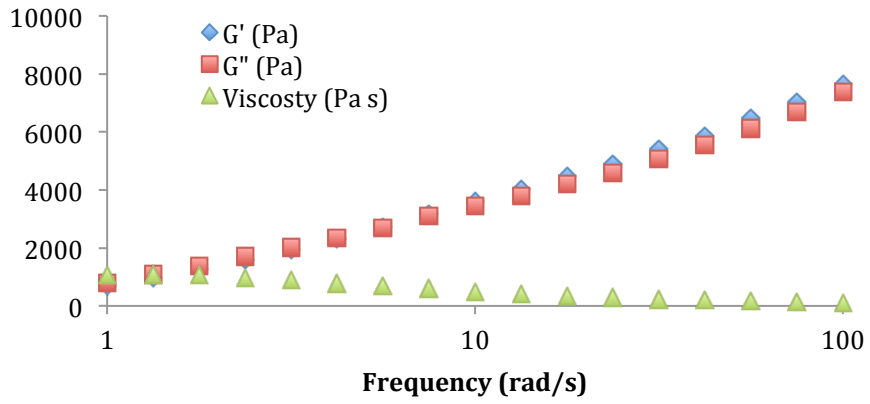

Figure 54. Dynamic frequency curve for $PNNP_{1100}$ 88:4:8 (300 mg/mL in PBS) at 37°C

As seen in the charts above, the viscoelastic properties of these materials are generally typical of a gel network, with storage modulus (G') much higher than loss modulus (G"), indicating a more elastic structure with greater association between molecules (Muller, et al. 1991). In many cases, moduli are seen to be more dependent on frequency than expected for a hydrogel system, indicating a more fluid-like material. This behavior could be due to difficulty in determining the linear viscoelastic region from dynamic strain curves. In most cases the dynamic strain curves indicate a linear viscoelastic region below one or two percent strain, although in some cases the region extends up to five percent strain. Materials with a longer and more easily identifiable linear viscoelastic region are likely to be more stable than those with a shorter linear viscoelastic region. From the dynamic frequency curves, we can see that the materials also exhibit shear-thinning characteristics, which may be beneficial for injection through small-gauge needles, as would be required for delivery to the posterior of the eye. These results also indicate that

the average moduli of the polymeric materials studied here is much higher than that of the average bovine or porcine vitreous, determined to be 32 and 10 Pa within 48 hours postmortem (Nickerson, et al. 2008). Similar viscoelastic studies of the human vitreous body are difficult to find, likely due to the challenges associated with timely dissection and assessment. For the proposed application, it is possible that higher viscosity materials might exhibit a stronger tamponade effect in cases where retinal detachment is involved, and so may be more desirable as a vitreous replacement. It may also be possible to reduce the moduli of the polymer solutions to better match the native vitreous by preparing a more dilute solution; further work could examine the effect that polymer concentration has on viscoelastic and other characteristics of these materials.

It is worth noting that as the temperature in the rheometer was controlled by means of a forced-air heating system, some evaporation of the sample likely occurred during testing. To mitigate these effects, readings were taken as quickly as possible after the chamber reached the required temperature. Incomplete heating of the material could have contributed to the difficulty encountered in determining the linear viscoelastic regions of some polymer systems, as the association of the molecules in solution is expected to increase above the LCST. Further work might examine other ways to mitigate evaporation effects, such as closed systems or other heating methods. While it may have been informative to include the viscoelastic properties of the materials at lower temperatures as well, available transducers were not capable of taking accurate readings, as the viscosities of the solutions were too low at room temperature.

4.2.6 Refractive Index

The refractive index of the vitreous has been determined by various methods to be approximately 1.336 (Schramm, et al. 2012). Based on the refractometer readings, the mean refractive index of the polymer solutions studied in this work was 1.37 at a temperature of 37°C. Refractive indices of the various polymer solutions are displayed in Figures 54 and 55 below.

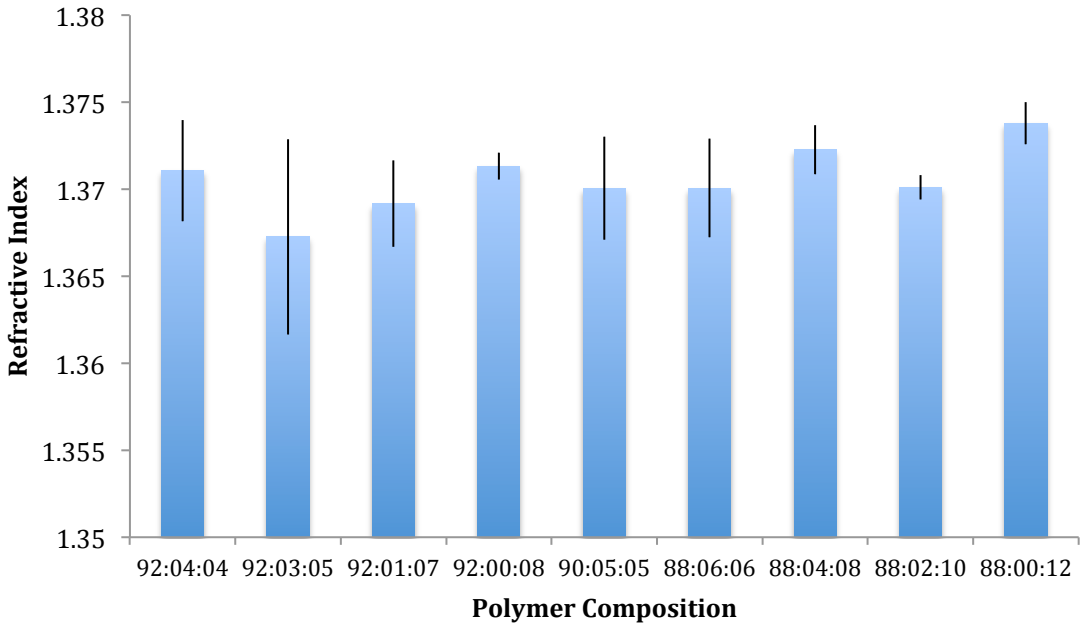

Figure 55. Refractive Indices of $PNNP_{1100/950}$ (300 mg/mL in PBS) at 37°C. Error bars represent standard deviation

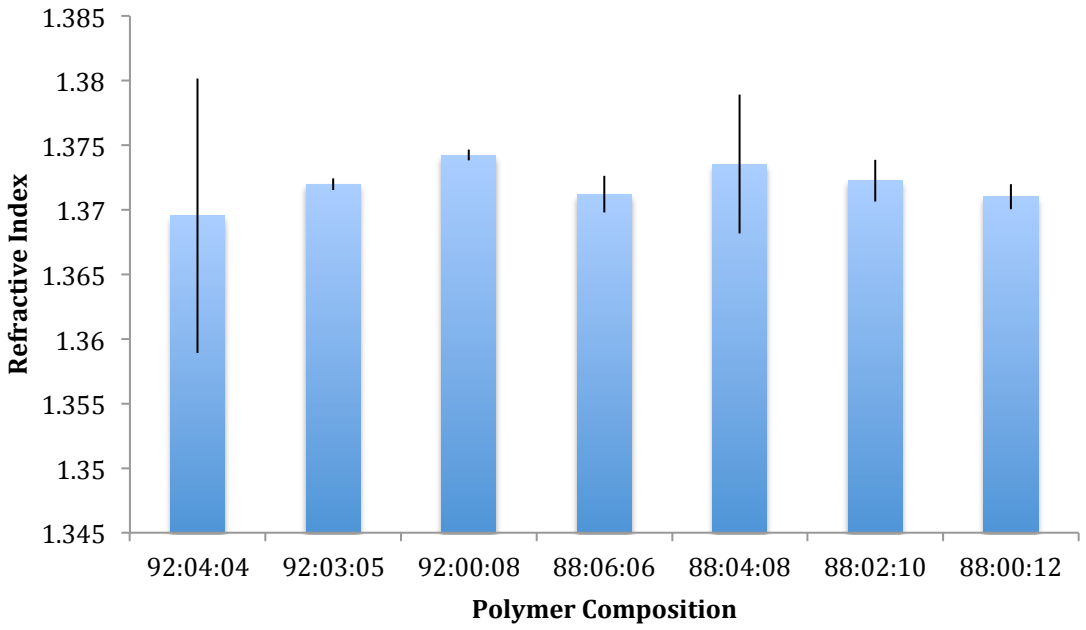

Figure 56. Refractive Indices of $PNNP_{475}$ (300 mg/mL in PBS) at 37°C. Error bars represent standard deviation

It is expected that more dilute solutions would exhibit lower refractive indices (Tang and Munkelwitz 1991), however high concentrations of polymer in solution were required for the formation of a solid gel. It is possible that these materials could be further modified to improve this characteristic; subsequent studies could incorporate methods to reduce the concentration at which gelation occurs and so potentially reduce the refractive index. Future studies could also investigate the feasibility of incorporating certain molecules that have been shown to reduce refractive index, such as fluorine (Soriano, Doma and Li 2009), into the polymer chain. Furthermore, the refractive index of these materials remains closer to that of the native vitreous than that of certain silicone compounds

currently used for vitreous replacements (Sparrow, et al. 1990); it may be possible to successfully utilize these materials without further modification of refractive properties.

4.2.7 Cellular Compatibility

In order to determine the potential cytotoxicity of the polymers, samples were incubated for a period of 24 hours with retinal pigment epithelial cells. Cell activity after these 24 hours was determined by MTT assay and compared to a control. These results are shown below.

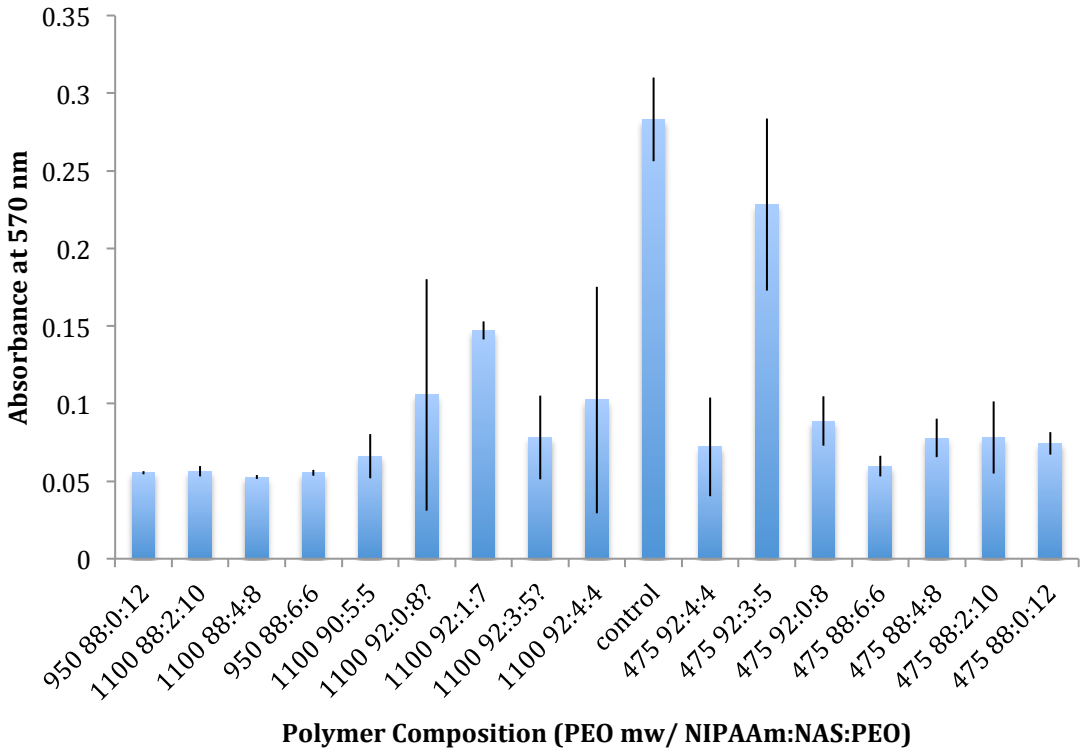

Figure 57. Cellular compatibility for 300 mg/mL PNNP after 24 hours by MTT assay. Error bars represent standard deviation

The results show significant cytotoxicity for most of the polymer formulations. This was unexpected, as similar polymer formulations have shown excellent cellular compatibility (Fitzpatrick 2012). From these results, cell viability does not appear to be correlated with

other polymer properties such as viscosity or molecular weight. While these results do not appear encouraging, it is important to note that the measured absorbance values for all test wells were quite low, indicating low cellular activity even in the control wells. This could be indicative of sub-optimal growth conditions that could be negatively affecting the results. As well, extensive polymer purification was not performed prior to incubation, and so significant improvements to the cytotoxic properties of the polymers are likely with extended dialysis to remove unreacted monomers from the mixture. There is a strong possibility that residual monomer could affect the results – NIPAAm in its unpolymerized form is known to be cytotoxic (Wadajkar, et al. 2009). In order to remove more of the residual monomer, additional precipitation steps or further dialysis of the polymer could be performed. Additionally, it is possible that the NAS groups have hydrolyzed to form acrylic acid, lowering the pH of the polymer solutions. This effect may be responsible for the observed colour change of the phenol red indicator used in the cell culture medium. To mitigate the effect this change has on cellular compatibility, it may be necessary to equilibrate the solutions before introduction to cells. It may also be possible that the high concentration of these polymers in solution is adversely affecting cell growth (Yeh, et al. 2006). Further work could attempt to minimize polymer concentration while optimizing the mechanical properties of the resulting gels in order to offset such detrimental effects. There also appears to be a weak correlation between the monomer feed ratio and cellular compatibility, with higher amounts of NIPAAm in the feed ratio resulting in increases to viability. Combined with more extensive treatment of

the polymer prior to cell introduction, this characteristic could be optimized to further reduce toxicity.

5.0 Conclusions

In this work, NIPAAm was co-polymerized with NAS and PEG in order to create a thermally-gelling polymer system. The resulting gels were then characterized to determine their potential as vitreous replacement materials. The results show that these materials may have some potential for artificial vitreous replacement. They are capable of forming viscous gels at physiological temperatures without the need for an activated cross linker. We have shown that they can provide adequate transparency in the visible spectrum and mechanical properties characteristic of more solid gel-like materials. It has been shown that the refractive index of these materials is higher than that of the native vitreous body, though not so high as to preclude it from use as artificial vitreous. Cellular compatibility studies show unexpectedly high toxicity levels. The measured level of toxicity is likely due to residual monomer content or pH imbalance, as similar polymers have been well tolerated both in-vivo and in-vitro. Further studies utilizing more extensive purification should be performed in order to obtain a better picture of how these polymers affect retinal cell growth. Additional studies should also examine the long-term stability of the polymers as well as investigating more consistent methods of characterizing LCST and molecular weight. Further work could also investigate the potential for a cloud point in the polymer solutions that might affect transparency.

6.0 Bibliography

Akiba, Jun, Norio Ueno, and Bireswar Chakrabarti. "Mechanisms of photo-induced vitreous liquefaction." *Current Eye Research*, 1994: 505-512.

Aliyar, Hyder, William Foster, Paul Hamilton, and Nathan Ravi. "Towards the development of an artificial human vitreous." *Polymer preprints* 45 (2004): 469-470.

Asua, José, et al. "Critically Evaluated Rate Coefficients for Free-Radical Polymerization, 5." *Macromolecular Chemistry and Physics* 205, no. 16 (2004): 2151-2160.

Baino, Francesco. "Towards an ideal biomaterial for vitreous replacement: Historical overview and future trends." *Acta Biomateriala* 7 (2011): 921-935.

Benson, William. "Familial Exudative Vitreoretinopathy." *Transactions of the American Ophthalmological Society* 93 (1995): 473-521.

Bishop, Paul. "Structural Macromolecules and Supramolecular organization of the Vitreous Gel." *Progress in retinal and eye research* 19, no. 3 (2000): 323-344.

Bishop, Paul, David Holmes, Karl Kadler, David McLeod, and Kees Bos. "Age-Related Changes on the Surface of Vitreous Collagen Fibrils." *Investigative Ophthalmology & Visual Science* 45, no. 4 (2004): 1041-1046.

Boettner, Edward, and J. Reimer Wolter. "Transmission of the ocular media." *Investigative Ophthalmology & Visual Science* 1, no. 6 (1962): 776-783.

Bos, K.J., D.F. Holmes, R.S. Meadows, K.E. Kadler, D. McLeod, and P.N. Bishop. "Collagen fibril organisation in mammalian vitreous by freeze etch/rotary shadowing electron microscopy." *Micron* 32, no. 3 (2001): 301-306.

Bromberg, Lev. "Properties of aqueous solutions and gels of poly(ethylene oxide)-b-poly(propylene oxide)-b-poly(ethylene oxide)-g-poly(acrylic acid)." *The Journal of Physical Chemistry B* 102, no. 52 (1998): 10736-10744.

Cavalieri, Francesca, Fausto Miano, Paulo D'Antona, and Gaio Paradossi. "Study of Gelling Behavior of Poly(vinyl alcohol)-Methacrylate for Potential Utilizations in Tissue Replacement and Drug Delivery." *Biomacromolecules* 5 (2004): 2439-2446.

Cabana, Alain, Abdellatif Aït-Kadi, and Julianna Juhász. "Study of the Gelation Process of Polyethylene Oxide –Polypropylene Oxideb –Polyethylene Oxide Copolymer (Poloxamer 407) Aqueous Solutions." *Journal of colloid and interface science* 190, no. 2 (1992): 307-312.

Cardillo, Jose, et al. "Post-traumatic proliferative vitreoretinopathy. The epidemiologic profile, onset, risk factors, and visual outcome." *Ophthalmology* 104, no. 7 (1997): 1166-1173.

Carlsson, Anders, Gunnar Karlström, and Björn Lindman. "Thermal gelation of nonionic cellulose ethers and ionic surfactants in water." *Colloids and Surfaces* 47 (1990): 147-165.

Chang, Tom, Christopher Pelzek, Randall Nguyen, Surendar Purohit, Garrett Scott, and Dawn Hay. "Inverted pneumatic retinopexy: A method of treating retinal detachments associated with inferior retinal breaks." *Ophthalmology* 110, no. 3 (2003): 589-594.

Chen, Xingwei, et al. "Chitosan-based thermosensitive hydrogel as a promising ocular drug delivery system: Preparation, characterization, and in vivo evaluation." *Journal of biomaterials applications*, 2011: 1-12.

Chen, Jyh-Ping, and Tai-Hong Cheng. "Functionalized temperature-sensitive copolymer for tissue engineering of articular cartilage and meniscus." *Colloids and Surfaces A: Physicochemical and Engineering Aspects* 313 (2008): 254-259.

Chirila, Traian, Ye Hong, Paul Dalton, Ian Constable, and Miguel Refojo. "The use of Hydrophilic Polymers as Artificial Vitreous." *Progress in Polymer Science* 23 (1998): 475-508.

Collier, Joel, et al. "Thermally and Photochemically Triggered Self-Assembly of Peptide Hydrogels." *Journal of the American Chemical Society* 123, no. 38 (2001): 9463-9464.

Comolli, Noelle, Birgit Neuhuber, Itzhak Fischer, and Anthony Lowman. "In vitro analysis of PNIPAAm–PEG, a novel, injectable scaffold for spinal cord repair." *Acta Biomateriala* 5 (2009): 1046-1055.

Cotlier, Edward, and Robert Weinreb. "Biocompatibility Assessment of Liquid Artificial Vitreous Replacements: Relevance of In Vitro Studies." *Survey of Ophthalmology* 52, no. 3 (2007): 289-299.

Dumortier, Gilles, Jean Louis Grossiord, Florence Agnely, and Jean Claude Chaumeil. "A review of poloxamer 407 pharmaceutical and pharmacological characteristics." *Pharmaceutical Research* 23, no. 12 (2006): 2709-2728.

Dailey, J.P., J.P. Phillips, C. Li, and J.S. Riffle. "Synthesis of silicone magnetic fluid for use in eye surgery." *Journal of magnetism and magnetic materials* 194, no. 1 (1999): 140-148.

Dalton, P.D., T.V. Chirila, Y. Hong, and A. Jefferson. "Oscillatory shear experiments as criteria for potential vitreous substitutes." *Polymer Gels and Networks* 3, no. 4 (1995): 429-444.

Drury, Brett, and Robert Bourke. "Short-term intraocular tamponade with perfluorocarbon heavy liquid." *British Journal of Ophthalmology* 95, no. 5 (2011): 694-698.

Fitzpatrick, Scott. *Minimally invasive copolymers for posterior segment ocular therapeutics.* Open access dissertations and theses, 2012, Paper 6996.

Ganachaud, François, Michael Monteiro, Robert Gilbert, Marie-Anne Dourges, San Thang, and Ezio Rizzardo. "Molecular weight characterization of poly (N-isopropylacrylamide) prepared by living free-radical polymerization." *Macromolecules* 33, no. 18 (2000): 6738-6745.

Gehrke, Stevin. "Synthesis, EquilibriumSwelling, Kinetics, Permeability and Applications of Environmentally Responsive Gels." *Responsive Gels: Volume Transitions II*, 1993: 81-144.

Gehroski, Dayle, and Henry Edelhauser. "Drug Delivery for Posterior Segment Eye Disease." *Investigative Ophthalmology & Visual Science* 41, no. 5 (2000): 961-964.

Goldbaum, Michael, Brooks McCuen, Anne Hanneken, Stuart Burgess, and Howard Chen. "Silicone Oil Tamponade to Seal Macular Holes without Position Restrictions." *Ophthalmology* 105, no. 11 (1998): 2140-2148.

Izunobi, Josephat, and Clement Higginbotham. "Polymer Molecular Weight Analysis by 1H NMR Spectroscopy." *Journal of Chemical Education* 88, no. 8 (2011): 1098-1104.

Hakin, Kim, Michael Lavin, and Peter Leaver. "Primary vitrectomy for rhegmatogenous retinal detachment." *Graefe's archive for clinical and experimental ophthalmology* 231, no. 6 (1993): 344-346.

Han, Y.K., J.W. Kwon, J.S. Kim, C-S. Cho, W.R. Wee, and J.H. Lee. "In vitro and in vivo study of lens refilling with poloxamer hydrogel." *British journal of ophthalmology* 87, no. 11 (2003): 1399-1402.

Han, Dennis, Naazli Mohsin, Clare Guse, Arthur Hartz, and Cynthia Tarkanian. "Comparison of Pneumatic Retinopexy and Scleral Buckling in the Management of Primary Rhegmatogenous Retinal Detachment." *American journal of ophthalmology* 126, no. 5 (1998): 658-668.

Hanyková, Lenka, Jan Labuta, and Jiří Spěváček. "NMR study of temperature-induced phase separation and polymer–solvent interactions in poly (vinyl methyl ether)/D2O/ethanol solutions." *Polymer* 47, no. 17 (2006): 6107-6116.

Heidenkummer, Hans-Peter, Anselm Kampik, and Sören Thierfelder. "Emulsification of silicone oils with specific physicochemical characteristics." *Graefe's archive for clinical and experimental ophthalmology* 229, no. 1 (1991): 88-94.

Holekamp, Nancy. "The Vitreous Gel: More than Meets the Eye." *American journal of ophthalmology* 149, no. 1 (2010): 32-36.

Hsiao, Meng-Hsuan, et al. "Design and characterization of a novel amphiphilic chitosan nanocapsule-based thermo-gelling biogel with sustained in vivo release of the hydrophilic anti-epilepsy drug ethosuximide." *Journal of Controlled Release* 161 (2012): 942-948.

Jung, David, Jon Paul Powers, Suzana Straus, and Robert Hancock. "Lipid-specific binding of the calcium-dependent antibiotic daptomycin leads to changes in lipid polymorphism of model membranes." *Chemistry and physics of lipids* 154, no. 2 (2008): 120-128.

Jyeong, Byeongmoon, Sung Wan Kim, and You Han Bae. "Thermosensitive sol–gel reversible hydrogels." *Advanced Drug Delivery Reviews* 64 (2012): 154-162.

Jongebloed, W.L., D. Humalda, and J.F.G. Worst. "A SEM-correlation of the anatomy of the vitreous body: Making visible the invisible." *Documenta Ophthalmalogica* 64, no. 1 (1986): 117-127.

Kikuchi, Akihiko, Mimako Kawabuchi, Masayasu Sugihara, Yasuhisa Sakurai, and Teruo Okano. "Pulsed dextran release from calcium-alginate gel beads." *Journal of controlled release* 47, no. 1 (1997): 21-29.

Kim, Soyeon, and Kevin Healy. "Synthesis and Characterization of Injectable Poly(N-isopropylacrylamide-co-acrylic acid) Hydrogels with Proteolytically Degradable Cross-Links." *Biomacromolecules* 4, no. 5 (2003): 1214-1223.

Le Goff, M.M., and P.N. Bishop. "Adult vitreous structure and postnatal changes." *Eye* 22, no. 10 (2008): 1214-1222.

Leaver, Peter. "Proliferative vitreoretinopathy." *The British journal of ophthalmology* 79, no. 10 (1995): 871-872.

Li, Zhenqing, Xiaolei Guo, Matsushita Satoshi, and Jianjun Guan. "Differentiation of cardiosphere-derived cells into a mature cardiac lineage using biodegradable poly(N-isopropylacrylamide) hydrogels." *Biomaterials* 32 (2011): 3220-3232.

Li, Chengming, Niklaas Buurma, Ihtshamul Haq, Colin Turner, and Steven Armes. "Synthesis and Characterization of Biocompatible, Thermoresponsive ABC and ABA Triblock Copolymer Gelators." *Langmuir* 21, no. 24 (2005): 11026-11033.

Lindgren, Gun, L. Sjödell, and Bertil Lindblom. "A prospective study of dense spontaneous vitreous hemorrhage." *American journal of ophthalmolog* 119, no. 4 (1995): 458.

Locke, John, and W. Ross Morton. "Further studies of the viscosity of aspirated human vitreous fluid: with special reference to its use in retinal detachment surgery." *Transactions of the American Ophthalmological Society* 63 (1965): 129-145.

Los, Leonoor, Roelofje van der Worp, Marja van Luyn, and Johanna Hooymans. "Age-Related Liquefaction of the Human Vitreous Body: LM and TEM Evaluation of the Role of Proteoglycans and Collagen." *Investigative ophthalmology & visual science* 44, no. 7 (2003): 2828-2833.

Nickerson, Charles, John Park, Julia Kornfield, and Hampar Karageozian. "Rheological properties of the vitreous and the role of hyaluronic acid." *Journal of Biomechanics* 41 (2008): 1840-1846.

Nisbet, D.R., et al. "Morphology and gelation of thermosensitive xyloglucan hydrogels." *Biophysical Chemistry* 121 (2006): 14-20.

Nishikawa, Shimpei, and Makoto Tamai. "Ultrastructure of hyaluronic acid and collagen in the human vitreous." *Current Eye Research*, 1995: 37-43.

Nitta, Yoko, and Katsuyoshi Nishinari. "Gelation and gel properties of polysaccharides gellan gum and tamarind xyloglucan." *International journal of biological macromolecules* 5, no. 3 (2005): 47-52.

Muller, René, Eric Gérard, Pascal Dugand, Paul Rempp, and Yves Gnanou. "Rheological Characterization of the Gel Point: A New Interpretation." *Macromolecules* 24, no. 6 (1991): 1321-1326.

Maruoka, Shinji, Toyoaki Matsuura, Kensuke Kawasaki, Masahiro Okamoto, and Hara Yoshiaki. "Biocompatibility of Polyvinylalcohol Gel as a Vitreous Substitute." *Current eye research* 31, no. 7-8 (2006): 599-606.

Messersmith, Phillip, and Steven Starke. "Thermally Triggered Calcium Phosphate Formation from Calcium-Loaded Liposomes." *Chemistry of materials* 10, no. 1 (1998): 117-124.

Miyazaki, S., S. Suzuki, N. Kawasaki, K. Endo, A. Takahashi, and D. Attwood. "In situ gelling xyloglucan formulations for sustained release ocular delivery of pilocarpine hydrochloride." *International Journal of Pharmaceutics* 229, no. 1 (2001): 29-36.

Miyazaki, Shozo, Fumie Suisha, Naoko Kawasaki, Mayumi Shirakawa, Kazuhiko Yamatoya, and David Attwood. "Thermally reversible xyloglucan gels as vehicles for rectal drug delivery." *Journal of Controlled Release* 56, no. 1 (1998): 75-83.

Miyamoto, Keifuku, Miguel Refojo, Filipe Tolentino, George Fournier, and Daniel Albert. "Fluorinated Oils as Experimental Vitreous Substitutes." *Archives of ophthalmology* 104, no. 7 (1986): 1053-1056.

Orrenius, Sten, Mark Burkitt, George Kass, Jeannette Dypbukt, and Pierluigi Nicotera. "Calcium ions and oxidative cell injury." *Annals of neurology* 32, no. S1 (1992): S33-S42.

Palmer, Warren, Eugene Emeson, and Thomas Johnston. "Poloxamer 407-induced atherogenesis in the C57BL:6 mouse." *Atherosclerosis* 136 (1998): 115-123.

Pastor, J. Carlos. "Proliferative Vitreoretinopathy: An Overview." *Survey of Ophthalmology* 43, no. 1 (1998): 3-18.

Pederson, Aaron, Jeffrey Ruberti, and Phillip Messersmith. "Thermal assembly of a biomimetic mineral/collagen composite." *Biomaterials* 24 (2003): 4881-4890.

Pritchard, Christopher, et al. "Evaluation of viscoelastic poly(ethylene glycol) sols as vitreous substitutes in an experimental vitrectomy model in rabbits." *Acta Biomateriala* 7 (2011): 936-943.

Procházka, Ondřej, and Pavel Kratochvíl. "An analysis of the accuracy of determining molar-mass averages of polymers by GPC with an on-line light-scattering detector." *Journal of Applied Polymer Science* 34, no. 6 (1987): 2325-2336.

Sanborn, Tracy, Phillip Messersmith, and Annelise Barron. "Insitucrosslinkingofabiomimeticpeptide-PEGhydrogelvia thermally triggered activation of factor XIII." *Biomaterials* 23 (2002): 2703-2710.

Sarkar, Nitis. "Thermal gelation properties of methyl and hydroxypropyl methylcellulose." *Journal of Applied Polymer Science* 24, no. 4 (2003): 1073-1087.

Schramm, Charlotte, et al. "The Cross-linked Biopolymer Hyaluronic Acid as an Artificial Vitreous Substitute." *Investigative Ophthalmology & Visual Science* 53, no. 2 (2012): 613-621.

Scott, John E. "The Chemical Morphology of the Vitreous." *Eye* 6 (1992): 553-555.

Sebag, J. "Age related changes in human vitreous structure." *Graefe's Archive for Clinical and Experimental Ophthalmology* 225 (1987): 89-93.

Sebag, J. "Anatomy and Pathology of the Vitreo-Retinal Interface." *Eye* 6 (1992): 541-552.

Sebag, J., and E.A. Balasz. "Morphology and Ultrastructure of Human Vitreous Fibers." *Investigative Ophthalmology & Visual Science* 30, no. 8 (1989): 1867-1871.

Shaw Jr, H.E., and M.B. Landers 3rd. "Vitreous hemorrhage after intracranial hemorrhage." *American journal of ophthalmology* 80, no. 2 (1975): 207.

Shirikawa, Mayumi, Kazuhiko Yamatoya, and Katsuyoshi Nishinari. "Tailoring of xyloglucan properties using an enzyme." *Food Hydrocolloids* 12, no. 1 (1998): 25-28.

Soman, N., and R. Banerjee. "Artificial vitreous replacements." *Bio-Medical Materials and Engineering* 13 (2003): 59-74.

Soriano, Allan, Bonifacio Doma, and Meng-Hui Li. "Measurements of the density and refractive index for 1-n-butyl-3-methylimidazolium-based ionic liquids." *The Journal of Chemical Thermodynamics* 41 (2009): 301-307.

Sparrow, Janet, Robert Ortiz, Peter MacLeish, and Stanley Chang. "ibroblast Behavior at Aqueous Interfaces with Perfluorocarbon, Silicone, and Fluorosilicone Liquids." *stigative Ophthalmology & Visual Science, Vo* 31, no. 4 (1990): 638-646.

Stenzer, Kurt, Michael Dunn, Albert Rubin, and Teruo Miyata. "Collagen Gels: Design for a Vitreous Replacement." *Science* 164, no. 3885 (1969): 1282-1283.

Stile, Ranee, Wesley Burghardt, and Kevin Healy. "Synthesis and Characterization of Injectable Poly(N-isopropylacrylamide)-Based Hydrogels That Support Tissue Formation in Vitro." *Macromolecules* 32 (1999): 7370-7379.

Ruel-Gariépy, E., A. Chenite, C. Chaput, S. Guirguis, and J.-C. Leroux. "Characterization of thermosensitive chitosan gels for the sustained delivery of drugs." *International Journal of Pharmaceutic* 203 (2000): 89-98.

Ruel-Gariépy, Eve, and Jean-Christophe Leroux. "In situ-forming hydrogels—review of temperature-sensitive systems." *European Journal of Pharmaceutics and Biopharmaceutics* 58 (2004): 409-426.

Turner, George. *Management of acute retinal detachment.* 2010/PROF/064, Ophthalmic Services Guidance, Manchester: The Royal College of Ophthalmologists, 2010.

Tang, I.N., and H.R. Munkelwitz. "Simultaneous determination of refractive index and density of an evaporating aqueous solution droplet." *Aerosol science and technology* 15, no. 3 (1991): 201-207.

Tate, Matthew, Deborah Shear, Stuart Hoffman, Donald Stein, and Michelle LaPlaca. "Biocompatibility of methylcellulose-based constructs designed for intracerebral gelation following experimental traumatic brain injury." *Biomaterials* 22, no. 10 (2001): 1113-1123.

Tefera, Nurelegne, Günter Weickert, Robert Bloodworth, and Johannes Schweer. "Free radical suspension polymerization kinetics of styrene up to high conversion." *Macromolecular Chemistry and Physics* 195, no. 9 (1994): 3067-3085.

Wadajkar, Aniket, Bhanuprasanth Koppolu, Maham Rahimi, and Kytai Nguyen. "Cytotoxic evaluation of N-isopropylacrylamide monomers and temperature-sensitive poly (N-isopropylacrylamide) nanoparticles." *Journal of Nanoparticle Research* 11, no. 6 (2009): 1375-1382.

Westhaus, Eric, and Phillip Messersmith. "Triggered release of calcium from lipid vesicles: a bioinspired strategy for rapid gelation of polysaccharide and protein hydrogels." *Biomaterials* 22 (2001): 453-462.

Wout, Zjumira, Edward Pec, Jack Maggiore, Robert Williams, Prema Palicharla, and Thomas Johnston. "Poloxamer 407—Mediated Changes in Plasma Cholesterol and Triglycerides Following Intraperitoneal Injection to Rats." *Journal of Pharmaceutical Science and Technology* 46, no. 6 (1992): 192-200.

Worst, Jan, and Leonoor Los. *Cisternal anatomy of the vitreous.* Kugler Publications, 1995.

Yeh, Judy, et al. "Micromolding of shape-controlled, harvestable cell-laden hydrogels." *Biomaterials* 27, no. 31 (2006): 5391–5398.